

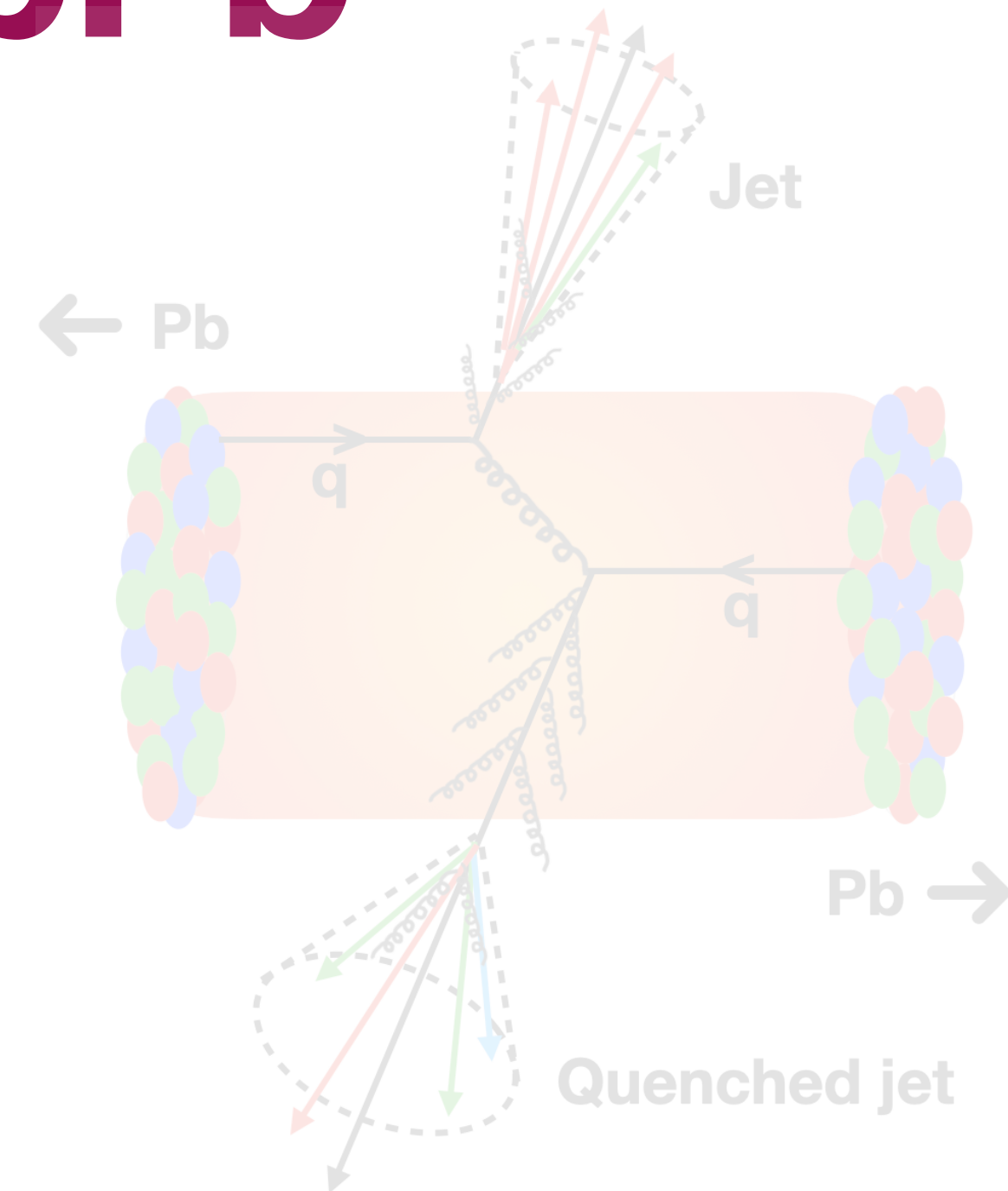
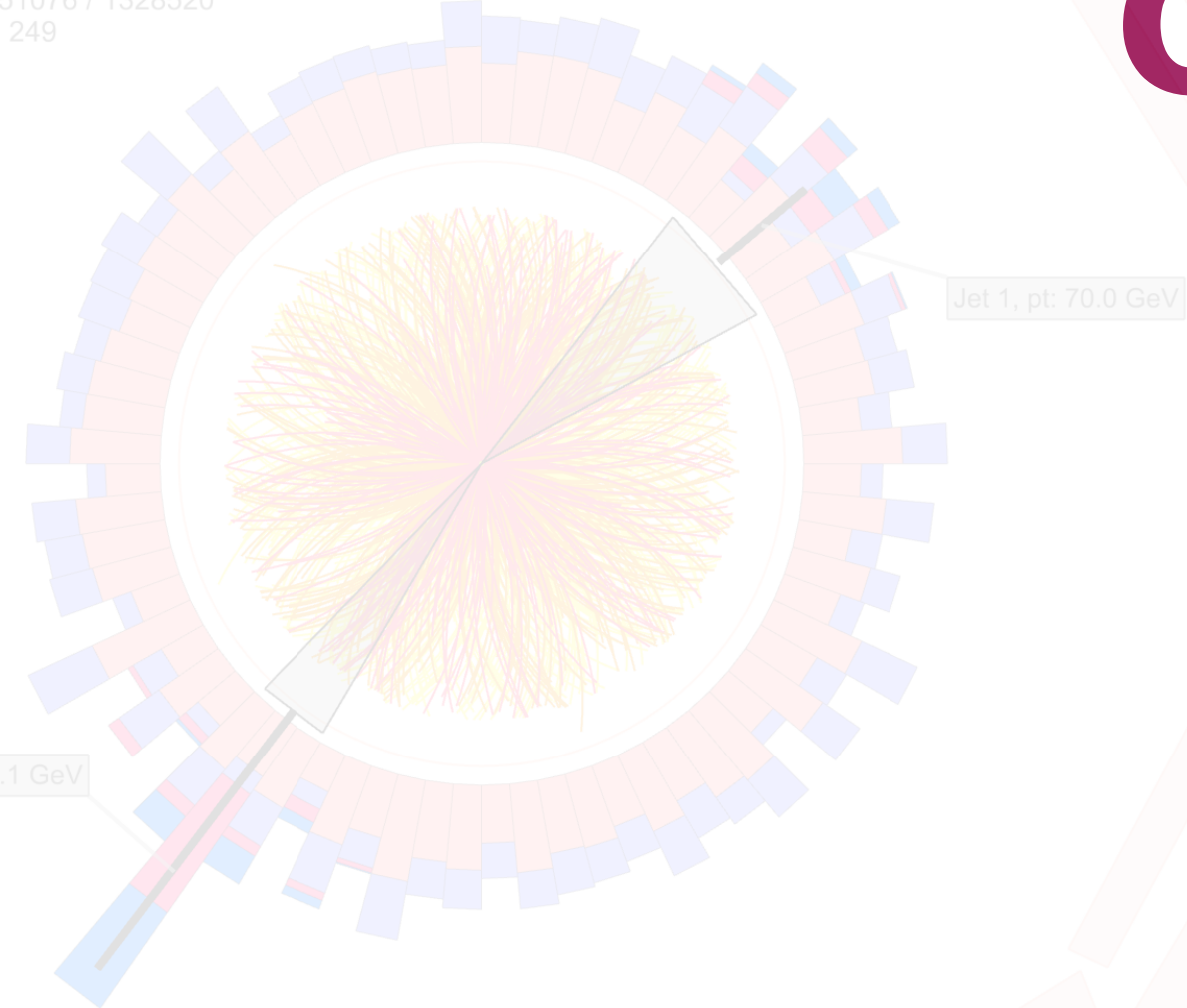
Constraining the color-charge effects of energy loss with jet axis-based substructure studies in PbPb collisions at 5.02 TeV

Raghunath Pradhan
for the CMS collaboration

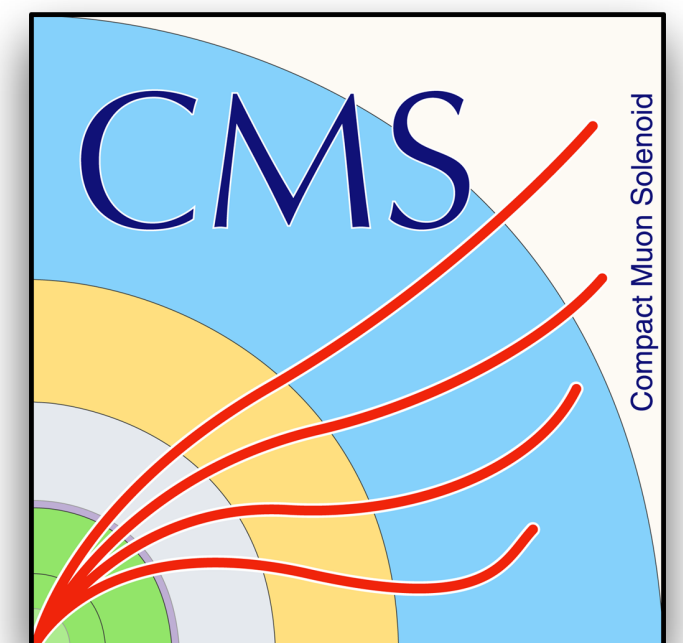
University of Illinois, Chicago

Date: 23/09/2024

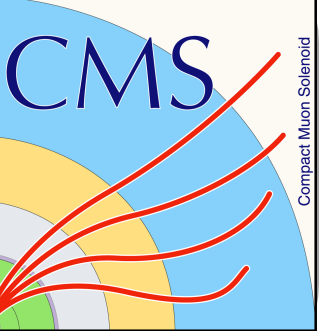
CMS Experiment at LHC, CERN
Data recorded: Sun Nov 14 19:31:39 2010 CEST
Run/Event: 151076 / 1328520
Lumi section: 249



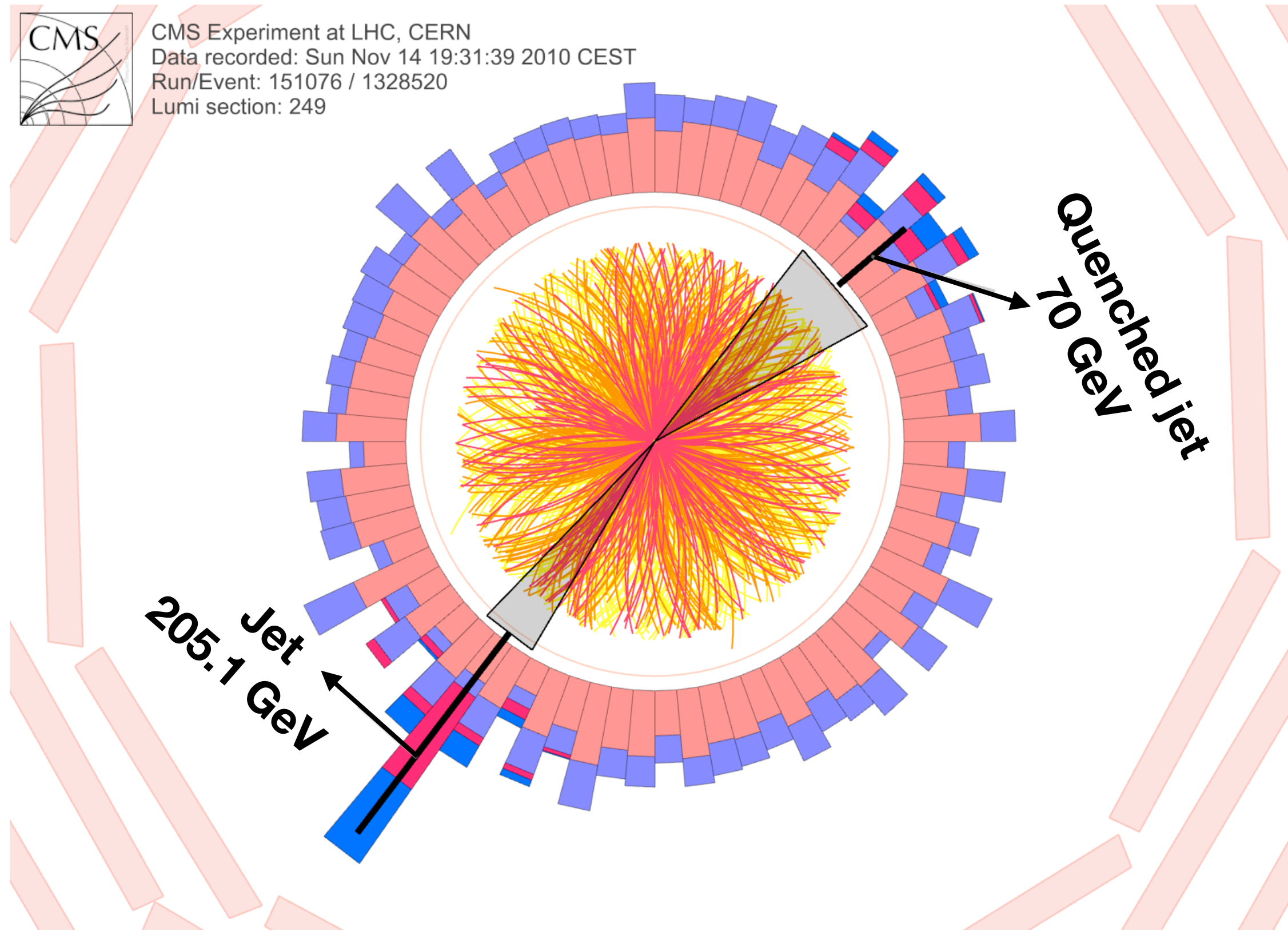
HP2024
N A G A S A K I



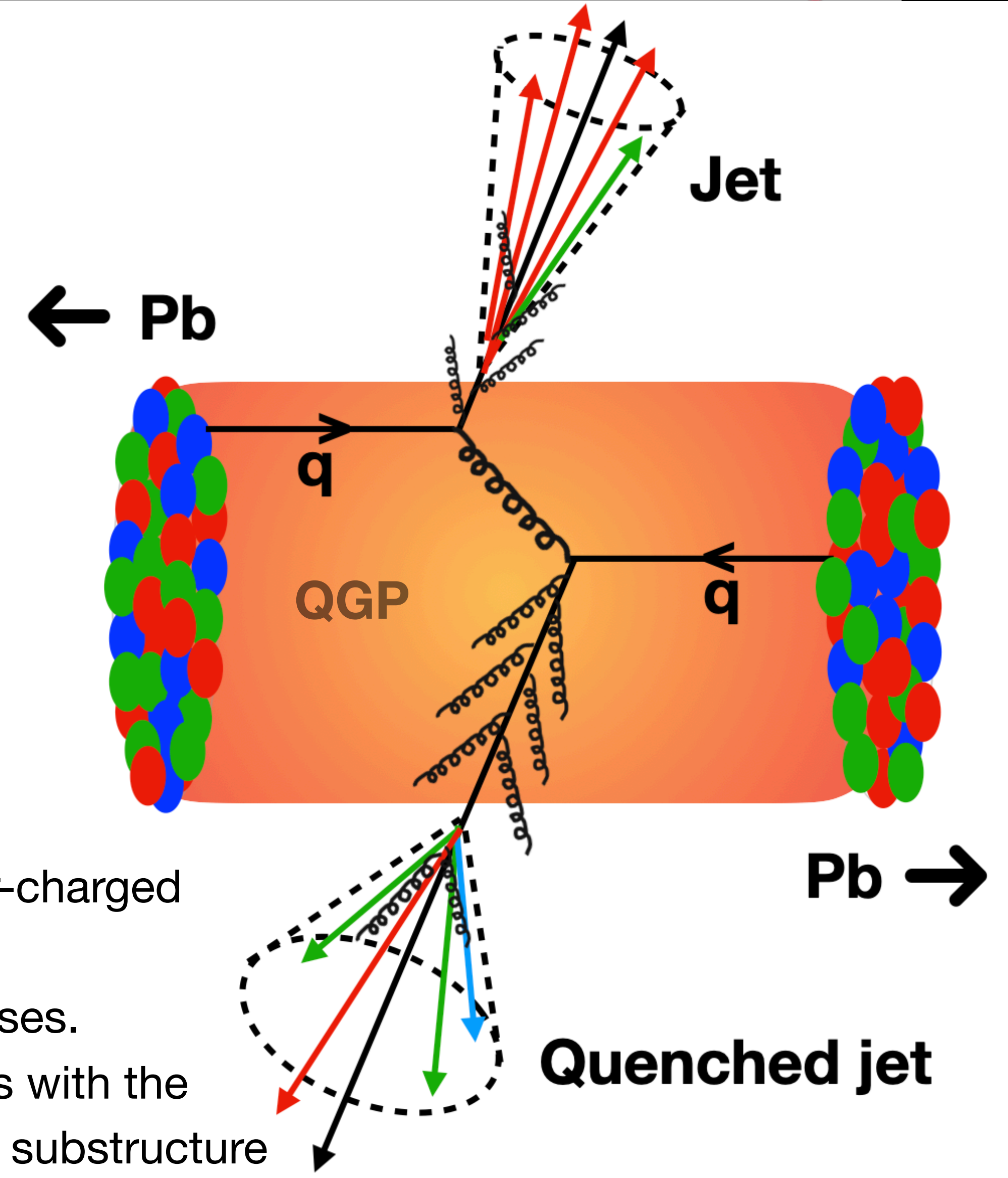
Introduction: QGP and jet quenching



CMS Experiment at LHC, CERN
Data recorded: Sun Nov 14 19:31:39 2010 CEST
Run/Event: 151076 / 1328520
Lumi section: 249



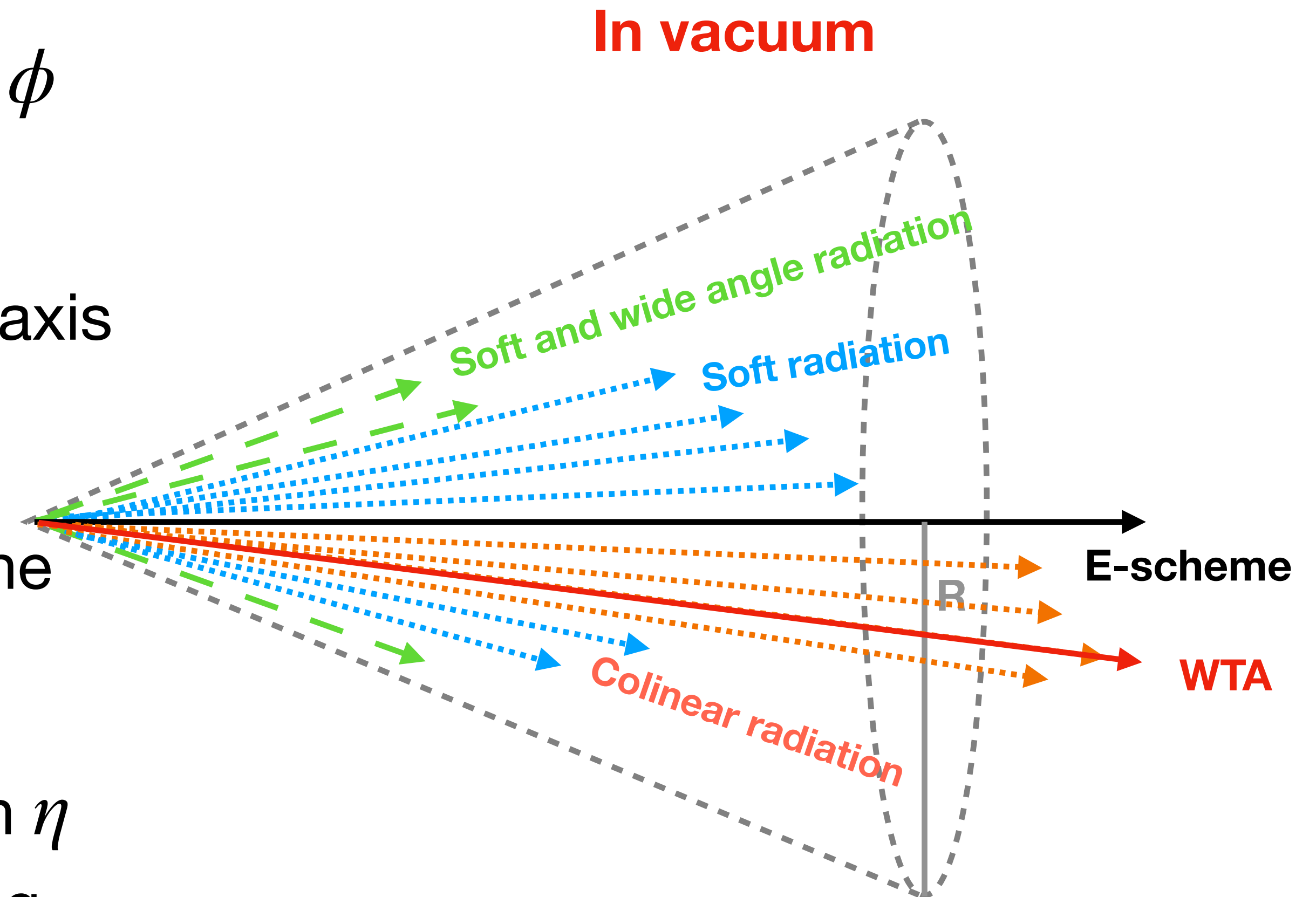
[Link](#)



- **Quark-Gluon Plasma (QGP):** A thermally equilibrated, deconfined color-charged state formed during the collision of two heavy nuclei.
- **Jet:** A collimated stream of particles produced in hard scattering processes.
- **Jet quenching:** The phenomenon where a jet loses energy as it interacts with the Quark-Gluon Plasma (QGP), leading to modifications in its structure and substructure

Introduction: jet axis

- Jet axis represents the direction of jet in η and ϕ coordinates
- This analysis focused on **E-scheme** and **WTA** axis
 - ▶ **E-scheme axis** : Coordinates in η and ϕ determined by the energy-weighted sum of the particle 4-momenta within a jet
 - ▶ **Winner-takes-all (WTA) axis** : Coordinates in η and ϕ representing the direction of the leading energy flow in a jet. Align with hard-collinear core of the jet



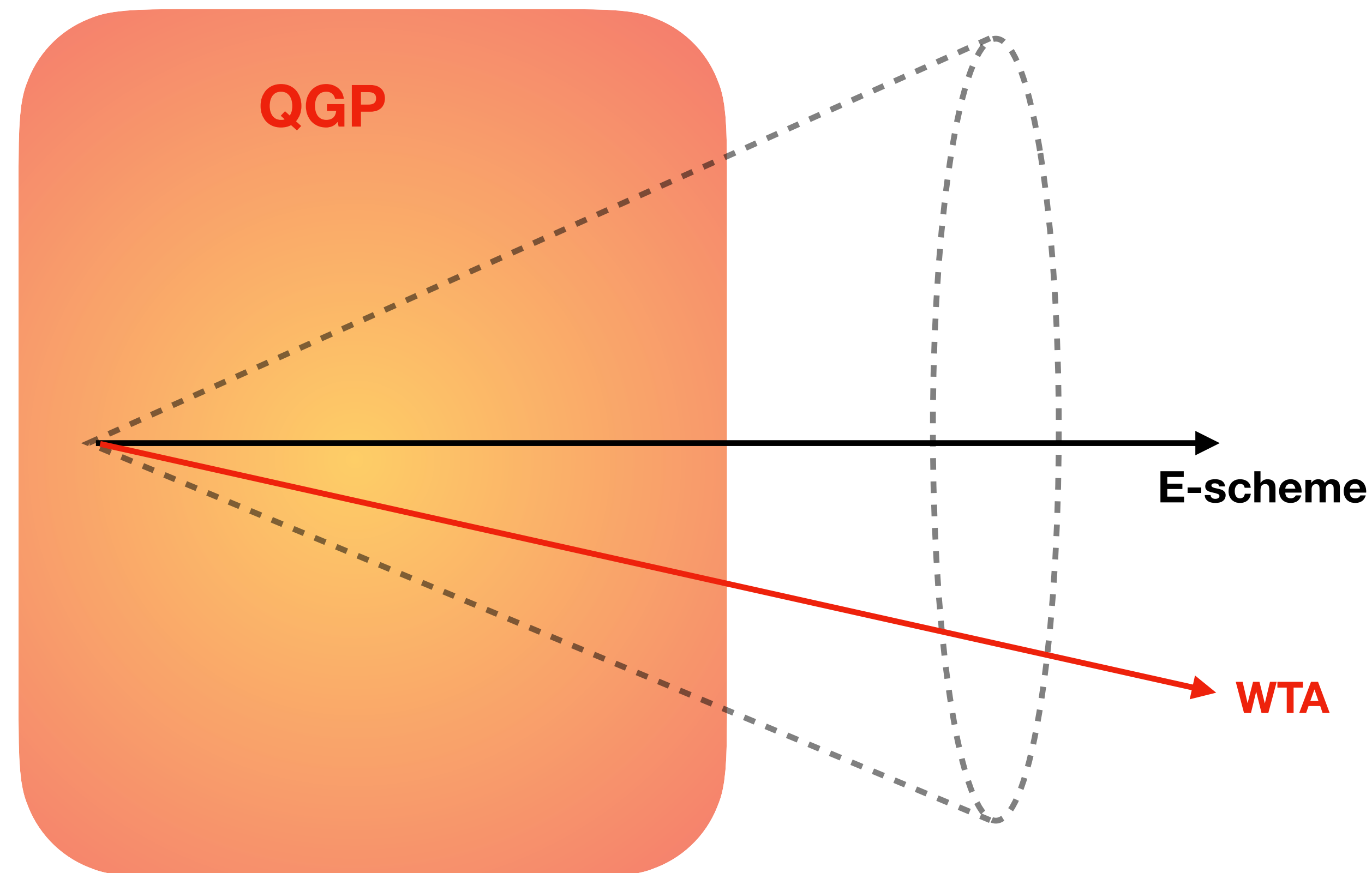
Introduction: jet axis

How the jet axes get modified in presence of medium?

For example:

- In medium gluon radiation can influencing the direction of **E-scheme axis**
- However, the **WTA axis** might be more susceptible to direction changes compared to the E-scheme axis if deflections of different jet partons go in random directions.

In the presence of a medium



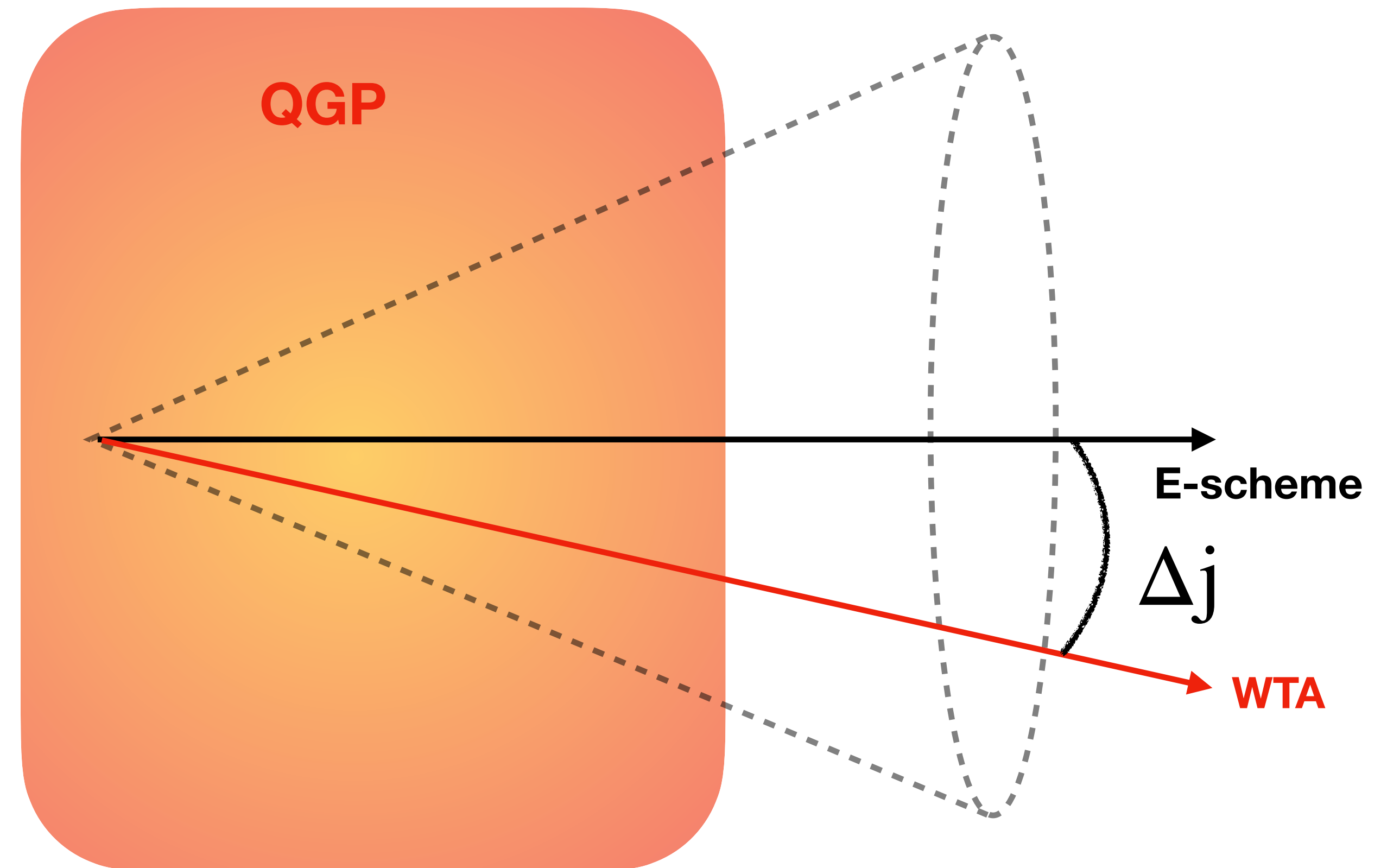
Introduction: angle between jet axis

How the jet axes get modified in presence of medium?

For example:

- In medium gluon radiation can influencing the direction of **E-scheme axis**
- However, the **WTA axis** might be more susceptible to direction changes compared to the E-scheme axis if deflections of different jet partons go in random directions.

In the presence of a medium



[JHEP04\(2020\)211](#)

Jet substructure observable $\Delta j = \sqrt{(\eta^{\text{E-scheme}} - \eta^{\text{WTA}})^2 + (\phi^{\text{E-scheme}} - \phi^{\text{WTA}})^2}$

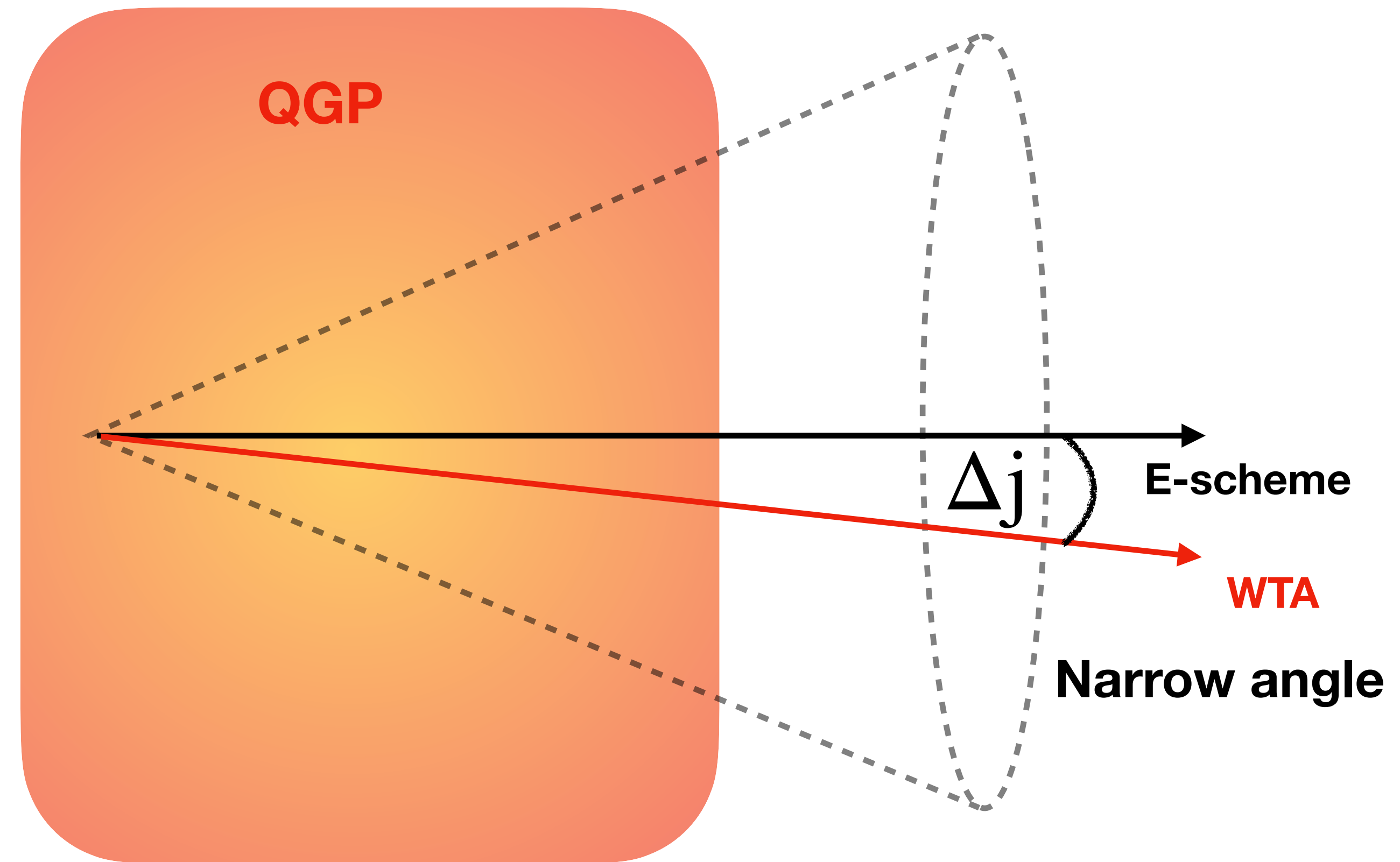
Introduction: angle between jet axis

How the jet axes get modified in presence of medium?

For example:

- In medium gluon radiation can influencing the direction of **E-scheme axis**
- However, the **WTA axis** might be more susceptible to direction changes compared to the E-scheme axis if deflections of different jet partons go in random directions.

In the presence of a medium



[JHEP04\(2020\)211](#)

Jet substructure observable $\Delta j = \sqrt{(\eta^{\text{E-scheme}} - \eta^{\text{WTA}})^2 + (\phi^{\text{E-scheme}} - \phi^{\text{WTA}})^2}$

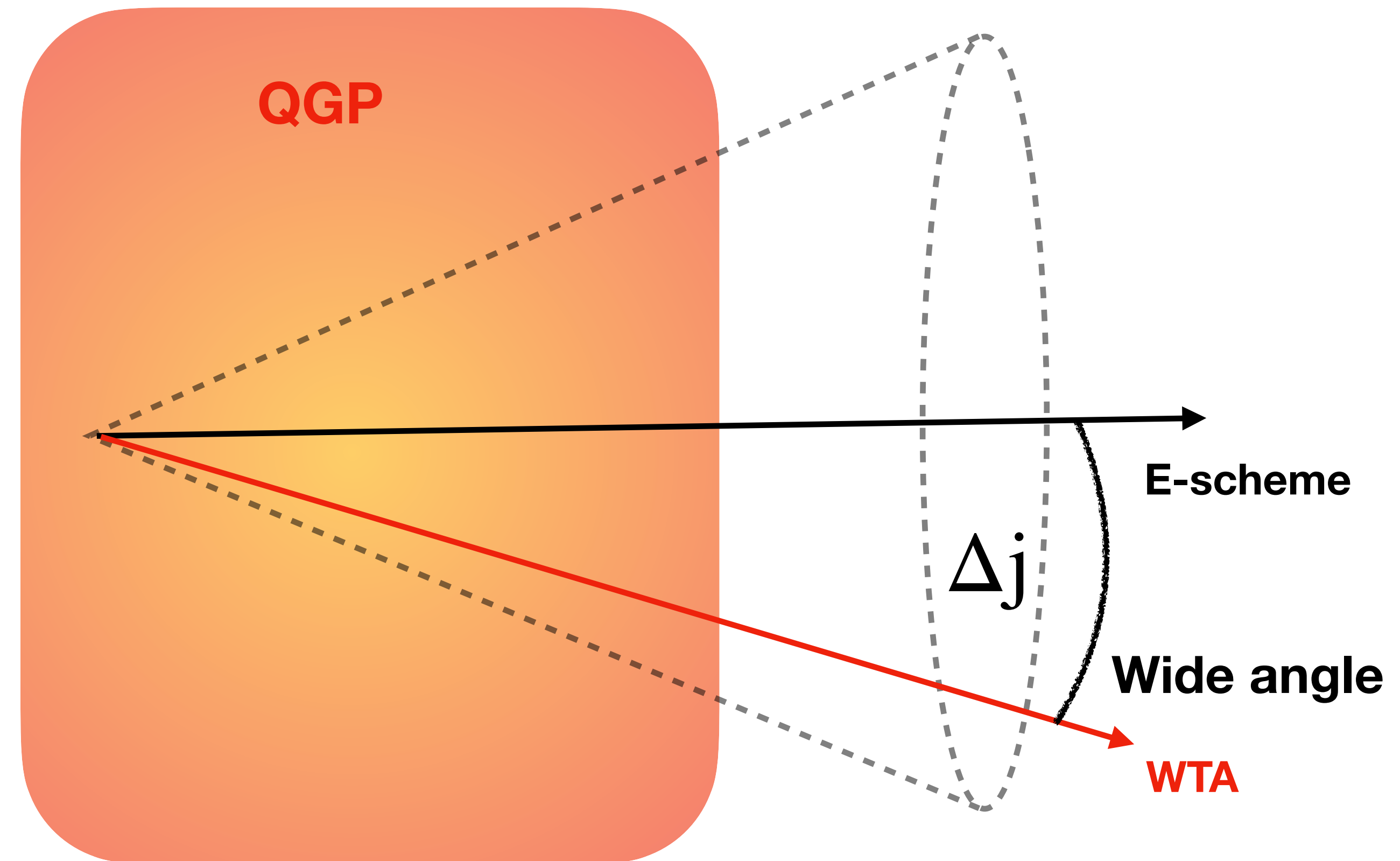
Introduction: angle between jet axis

How the jet axes get modified in presence of medium?

For example:

- In medium gluon radiation can influencing the direction of **E-scheme axis**
- However, the **WTA axis** might be more susceptible to direction changes compared to the E-scheme axis if deflections of different jet partons go in random directions.

In the presence of a medium



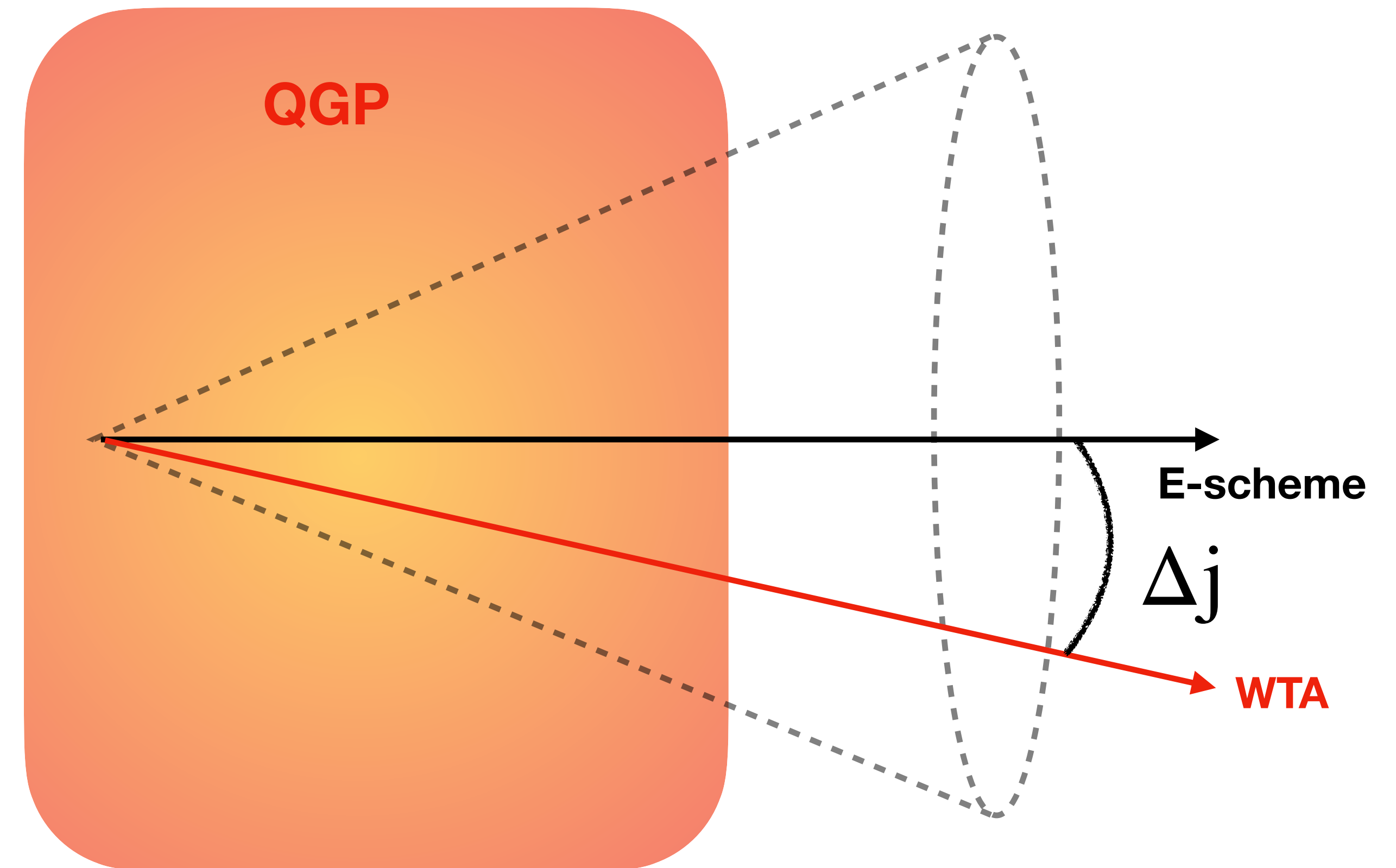
[JHEP04\(2020\)211](#)

Jet substructure observable $\Delta j = \sqrt{(\eta^{\text{E-scheme}} - \eta^{\text{WTA}})^2 + (\phi^{\text{E-scheme}} - \phi^{\text{WTA}})^2}$

Search for QGP induced jet substructure modification

- The correlation between **E-scheme** and **WTA axis** is used to access jet substructure
- ▶ Boost invariant and analytical calculation possible ([JHEP04\(2020\)211](#))
- ▶ Could provide insights into radiative energy loss in QGP, as the E-scheme and WTA axis exhibit different sensitivities to soft radiation
- ▶ Sensitive to various medium-induced effects

In the presence of a medium



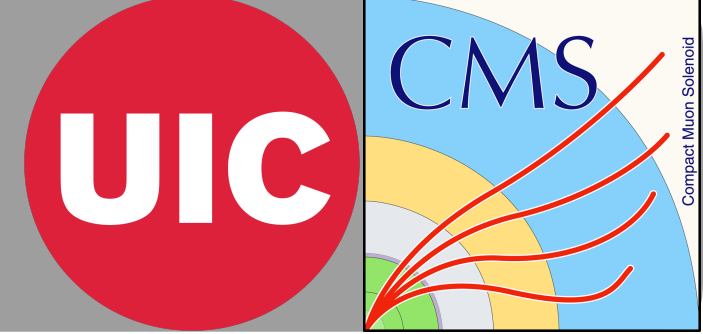
Jet substructure observable

$$\Delta j = \sqrt{(\eta^{\text{E-scheme}} - \eta^{\text{WTA}})^2 + (\phi^{\text{E-scheme}} - \phi^{\text{WTA}})^2}$$

2018 PbPb data at 5.02 TeV

- Centrality: 0-80%
- Centrality binning: {0, 10, 30, 50, 80}%
- Anti- k_T $R = 0.4$
- $|\eta^{\text{jet}}| < 1.6$
- $120 < p_T^{\text{jet}} < 300$ GeV
- p_T^{jet} binning: {120, 150, 190, 230, 300} GeV

Analysis set up and CMS detector

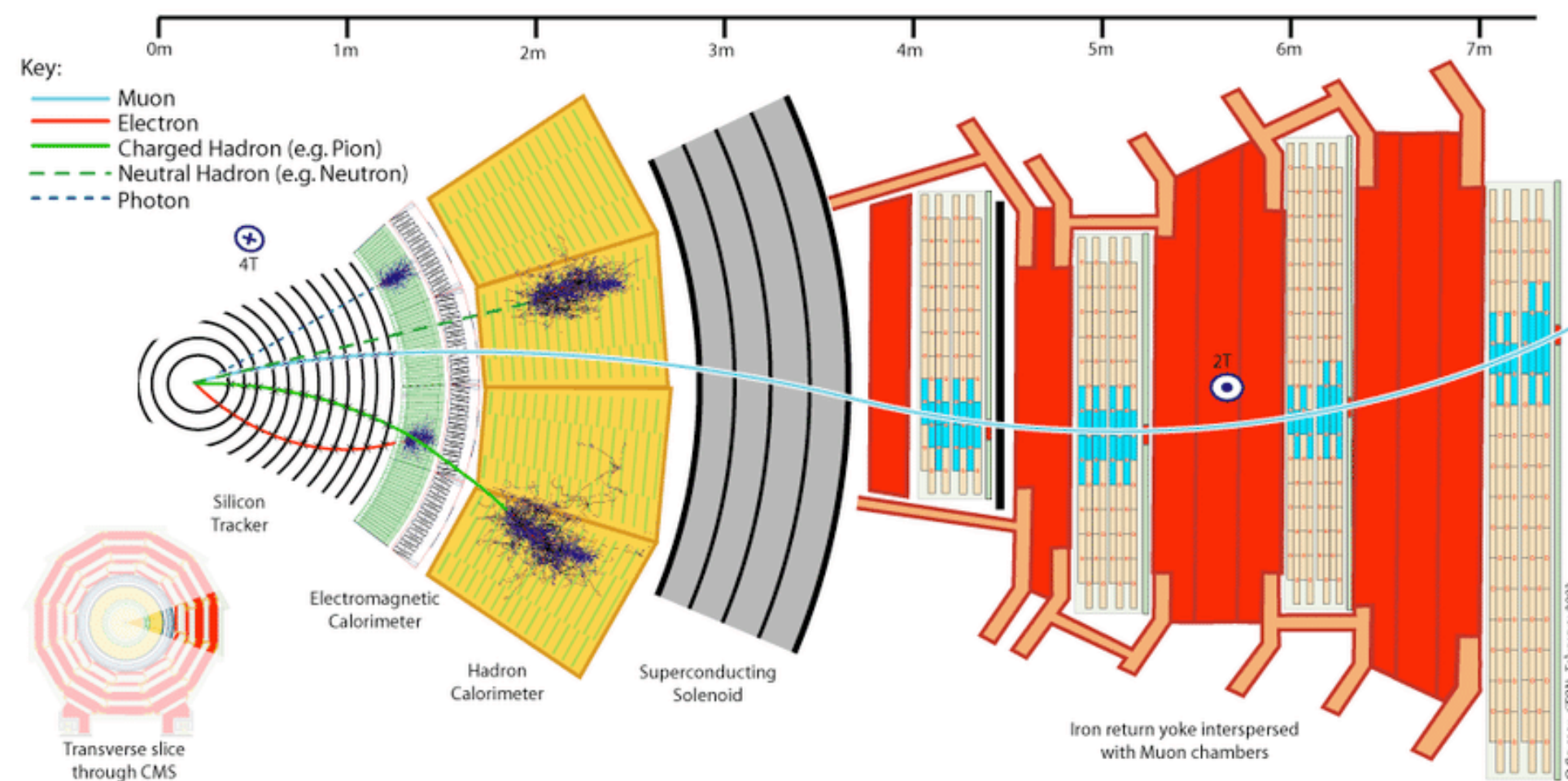


2018 PbPb data at 5.02 TeV

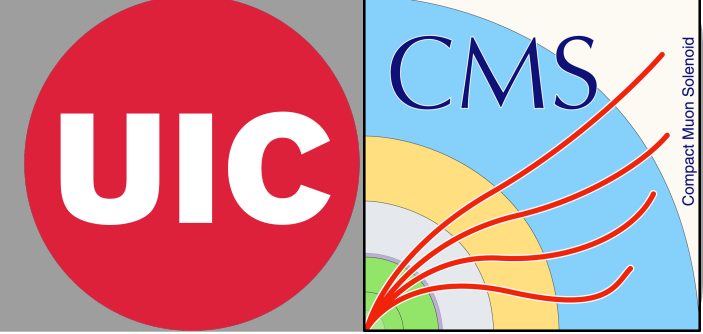
- Centrality: 0-80%
- Centrality binning: {0, 10, 30, 50, 80}%
- Anti- k_T $R = 0.4$
- $|\eta^{\text{jet}}| < 1.6$
- $120 < p_T^{\text{jet}} < 300$ GeV
- p_T^{jet} binning: {120, 150, 190, 230, 300} GeV

- Particle flow candidates used to reconstruct jets [Link](#)

Cross-sectional view
of the CMS detector



Analysis set up and CMS detector

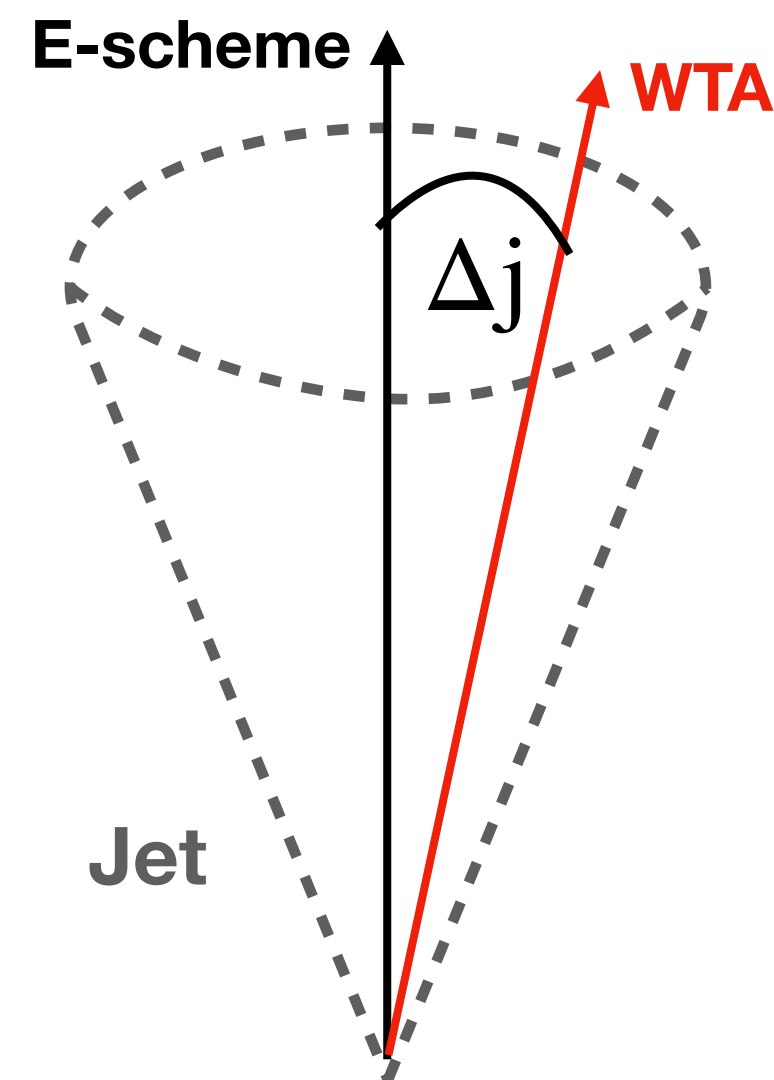


2018 PbPb data at 5.02 TeV

- Centrality: 0-80%
- Centrality binning: {0, 10, 30, 50, 80}%
- Anti- k_T $R = 0.4$
- $|\eta^{\text{jet}}| < 1.6$
- $120 < p_T^{\text{jet}} < 300$ GeV
- p_T^{jet} binning: {120, 150, 190, 230, 300} GeV

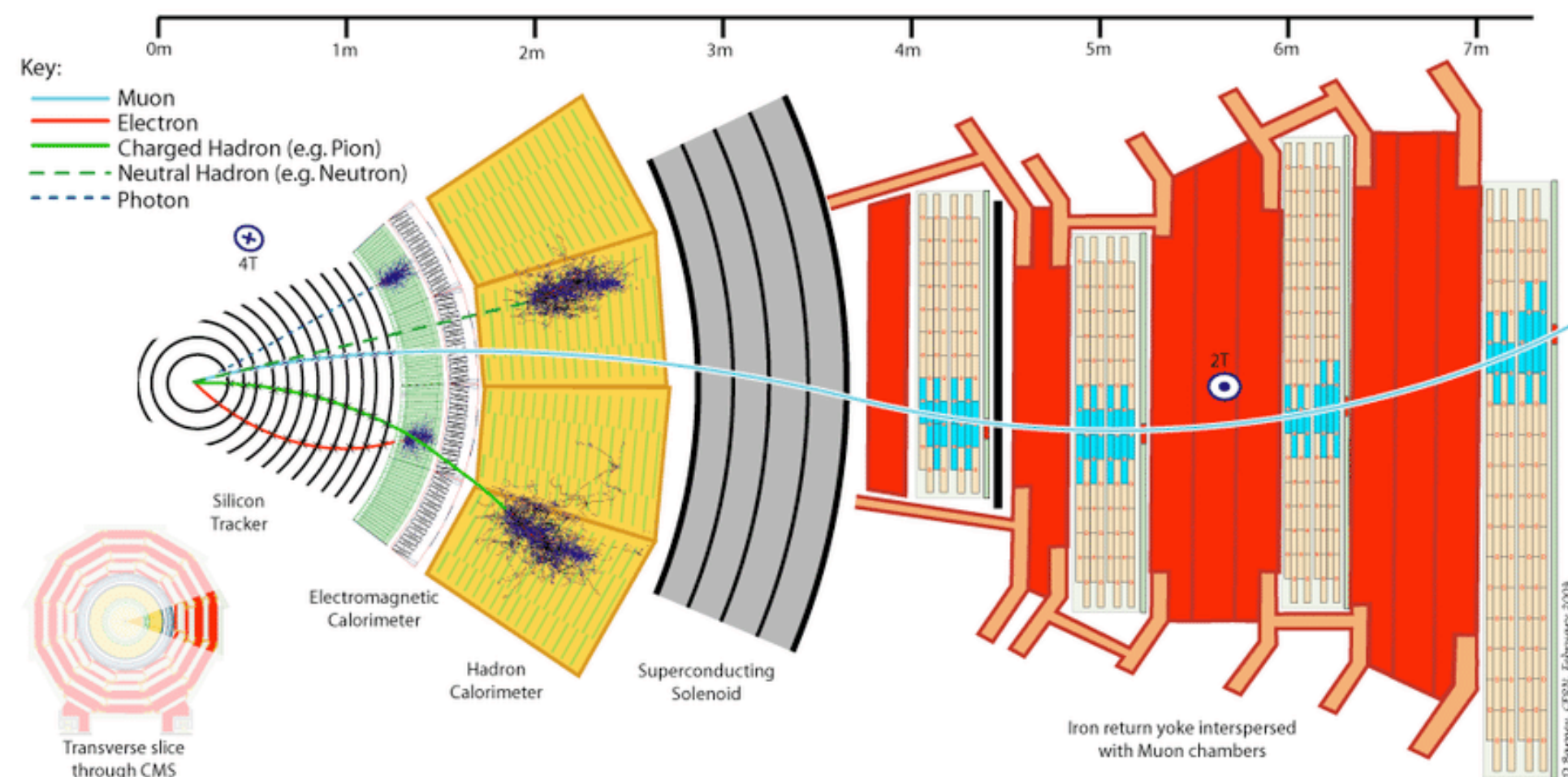
$$\text{Observable } \Delta j = \sqrt{(\eta^{\text{E-scheme}} - \eta^{\text{WTA}})^2 + (\phi^{\text{E-scheme}} - \phi^{\text{WTA}})^2}$$

Normalised $\rightarrow \frac{1}{N} \frac{dN}{d\Delta j}$, $N = \text{total number of jets}$



- Particle flow candidates used to reconstruct jets [Link](#)

Cross-sectional view of the CMS detector



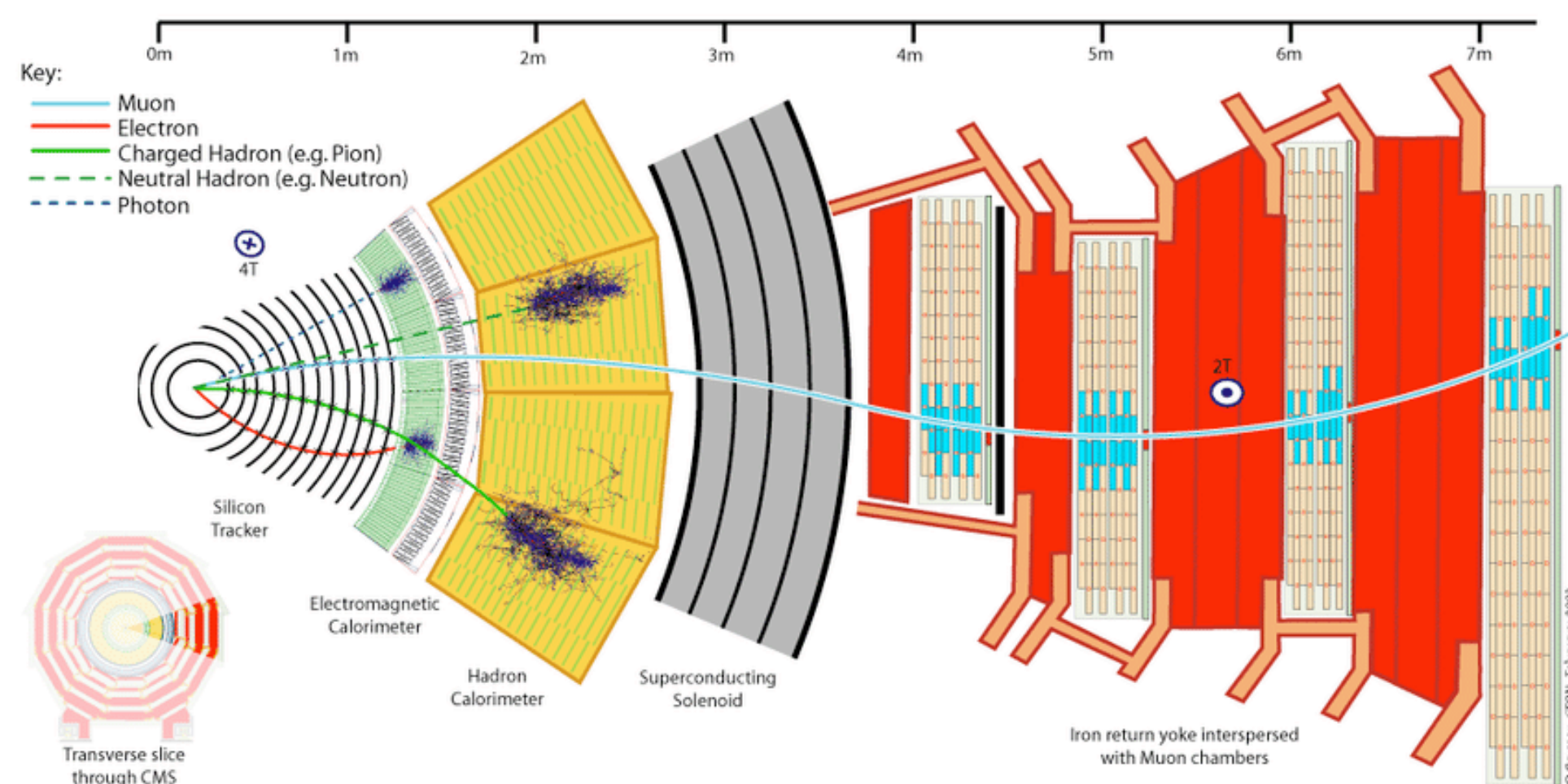
Analysis set up and CMS detector

2018 PbPb data at 5.02 TeV

- Centrality: 0-80%
- Centrality binning: {0, 10, 30, 50, 80}%
- Anti- k_T $R = 0.4$
- $|\eta^{\text{jet}}| < 1.6$
- $120 < p_T^{\text{jet}} < 300$ GeV
- p_T^{jet} binning: {120, 150, 190, 230, 300} GeV

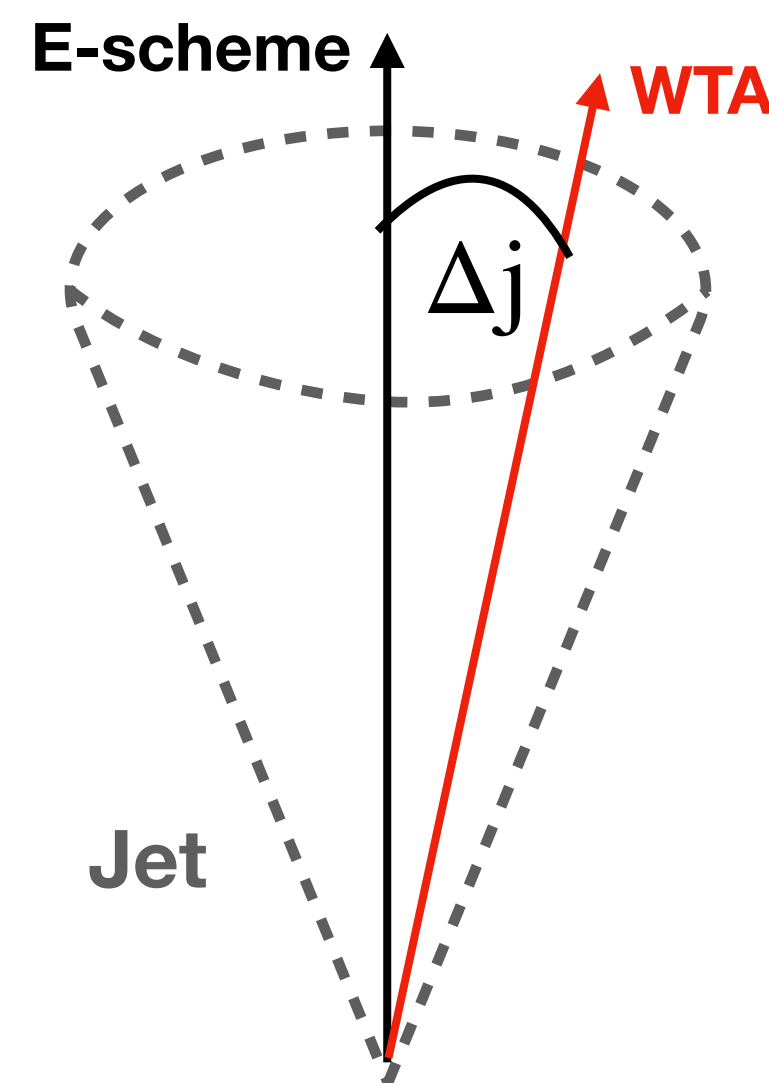
- Particle flow candidates used to reconstruct jets [Link](#)

Cross-sectional view of the CMS detector



Observable $\Delta j = \sqrt{(\eta^{\text{E-scheme}} - \eta^{\text{WTA}})^2 + (\phi^{\text{E-scheme}} - \phi^{\text{WTA}})^2}$

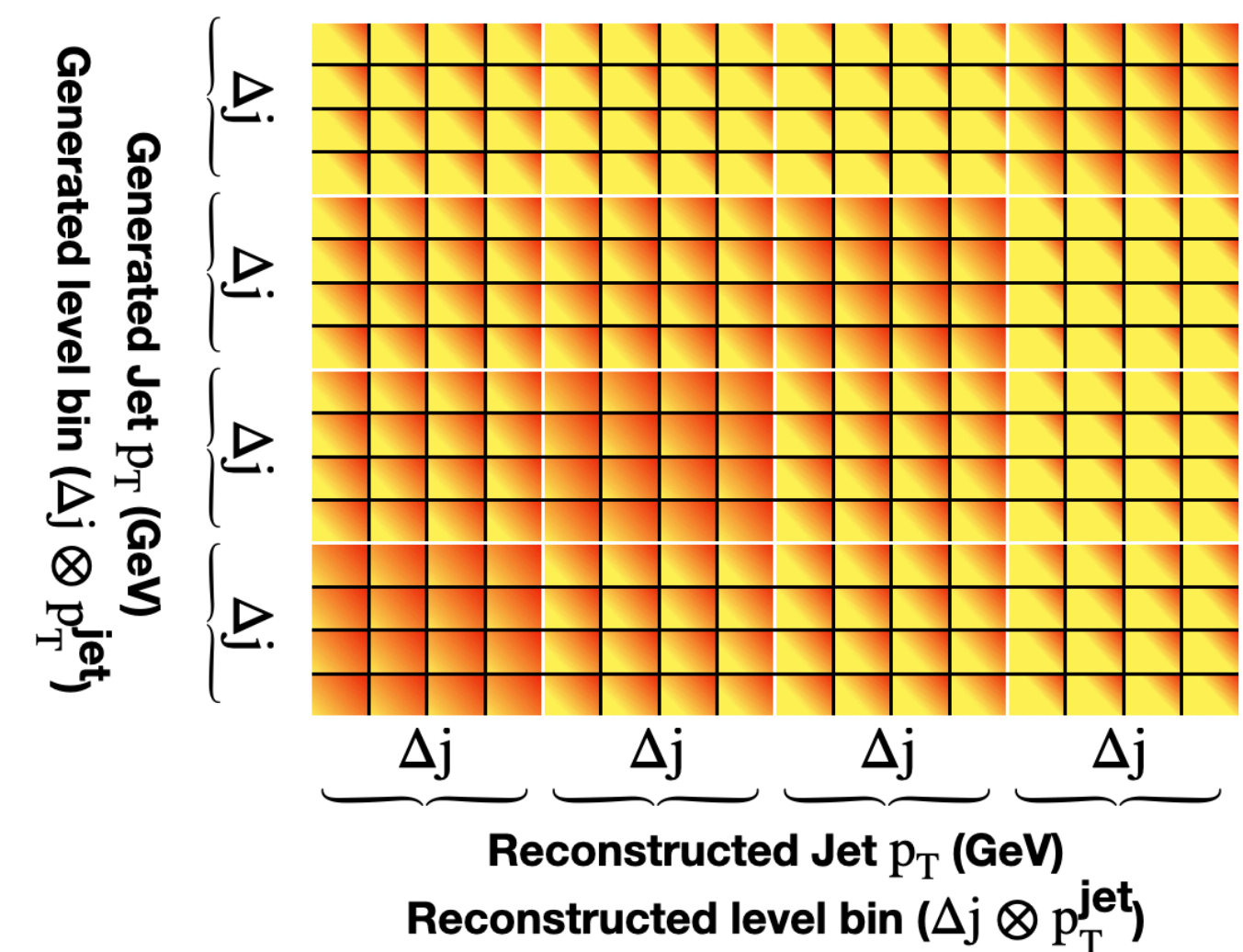
Normalised $\rightarrow \frac{1}{N} \frac{dN}{d\Delta j}$, $N = \text{total number of jets}$



Unfolding procedure

- Method: D' Agostini iterative
- Unfold two-dimensionally in p_T^{jet} and Δj

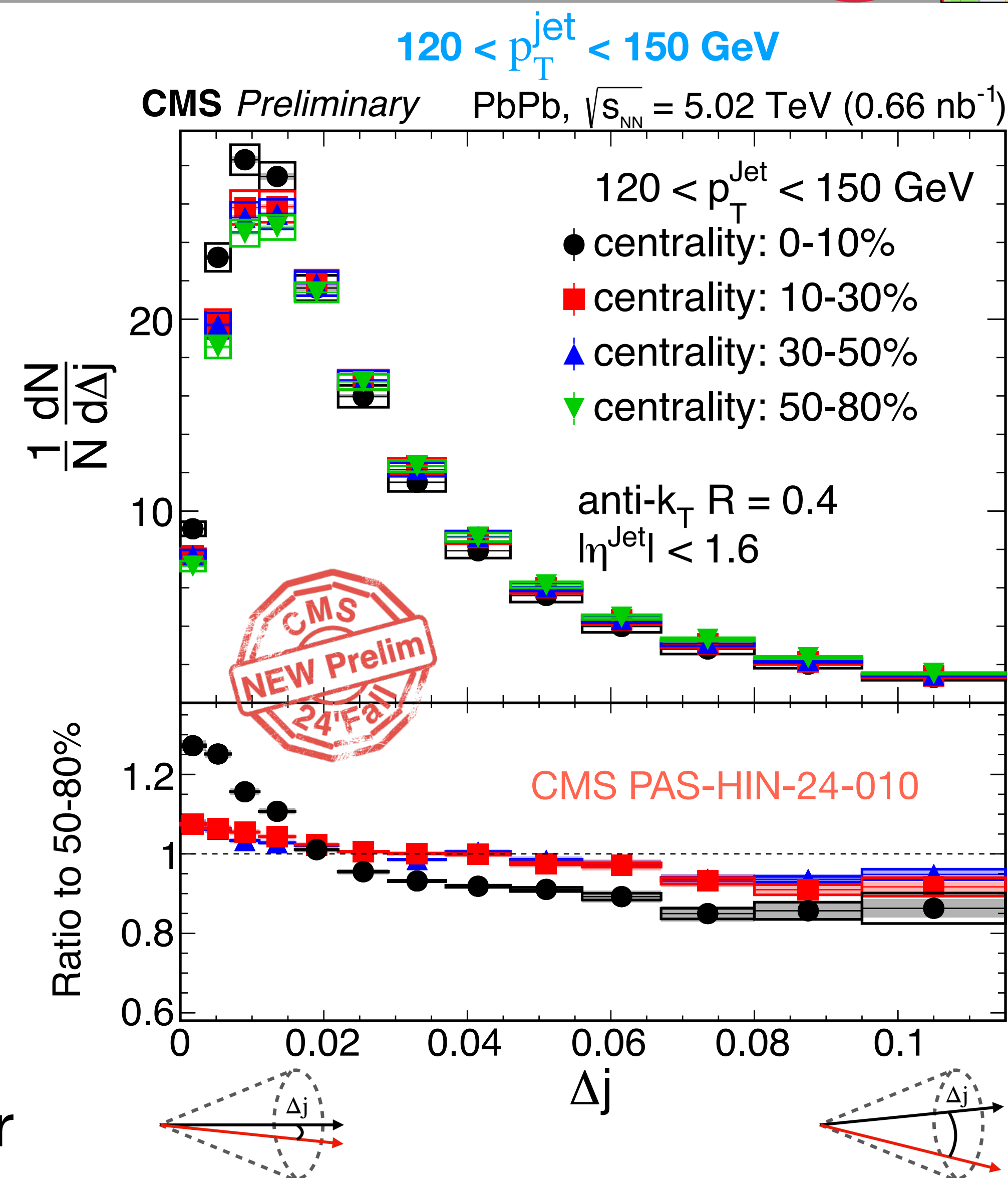
Response matrix cartoon \rightarrow



Results: unfolded Δ_j distributions

- Relative enhancement at lower Δ_j and suppression at higher Δ_j
- The Δ_j distributions in central collisions is narrower than peripheral collisions
- Applied cancelation of the correlated systematic error in the ratio

- Correlated systematic error
- Uncorrelated systematic error



Results: in higher p_T^{jet} bins

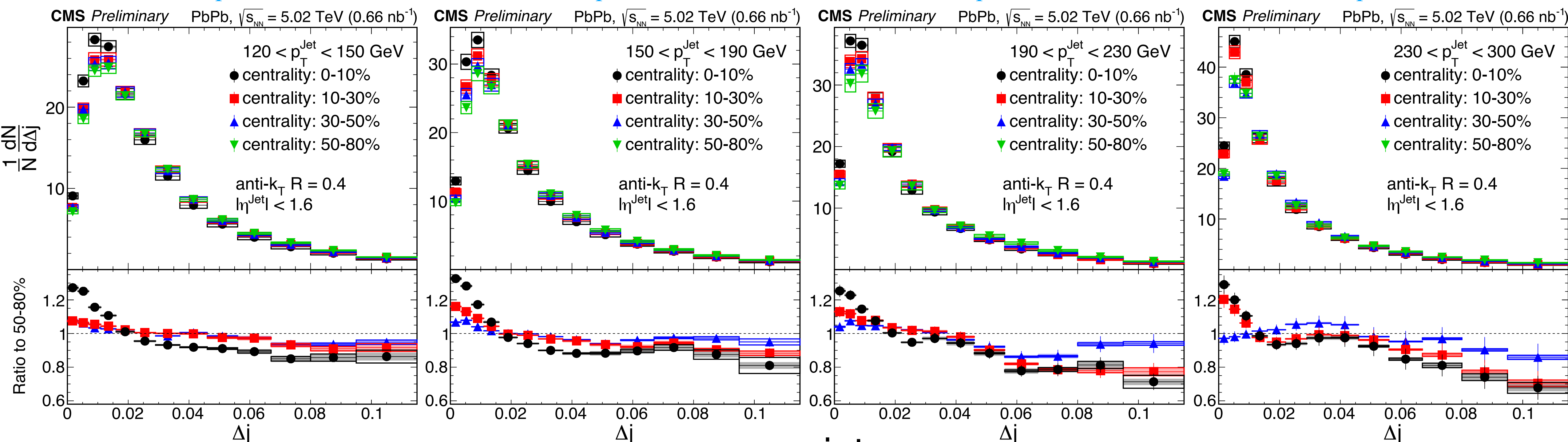
Increasing p_T^{jet}

$120 < p_T^{\text{jet}} < 150 \text{ GeV}$

$150 < p_T^{\text{jet}} < 190 \text{ GeV}$

$190 < p_T^{\text{jet}} < 230 \text{ GeV}$

$230 < p_T^{\text{jet}} < 300 \text{ GeV}$

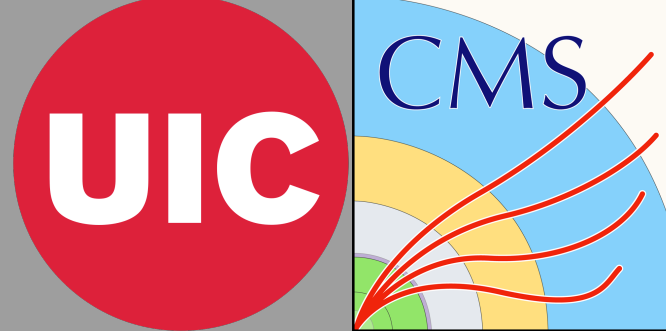


- Narrowing behaviour observed in all the p_T^{jet} bins studied in this analysis
 - modification of jet substructure and/or selection bias due to p_T^{jet} selection?

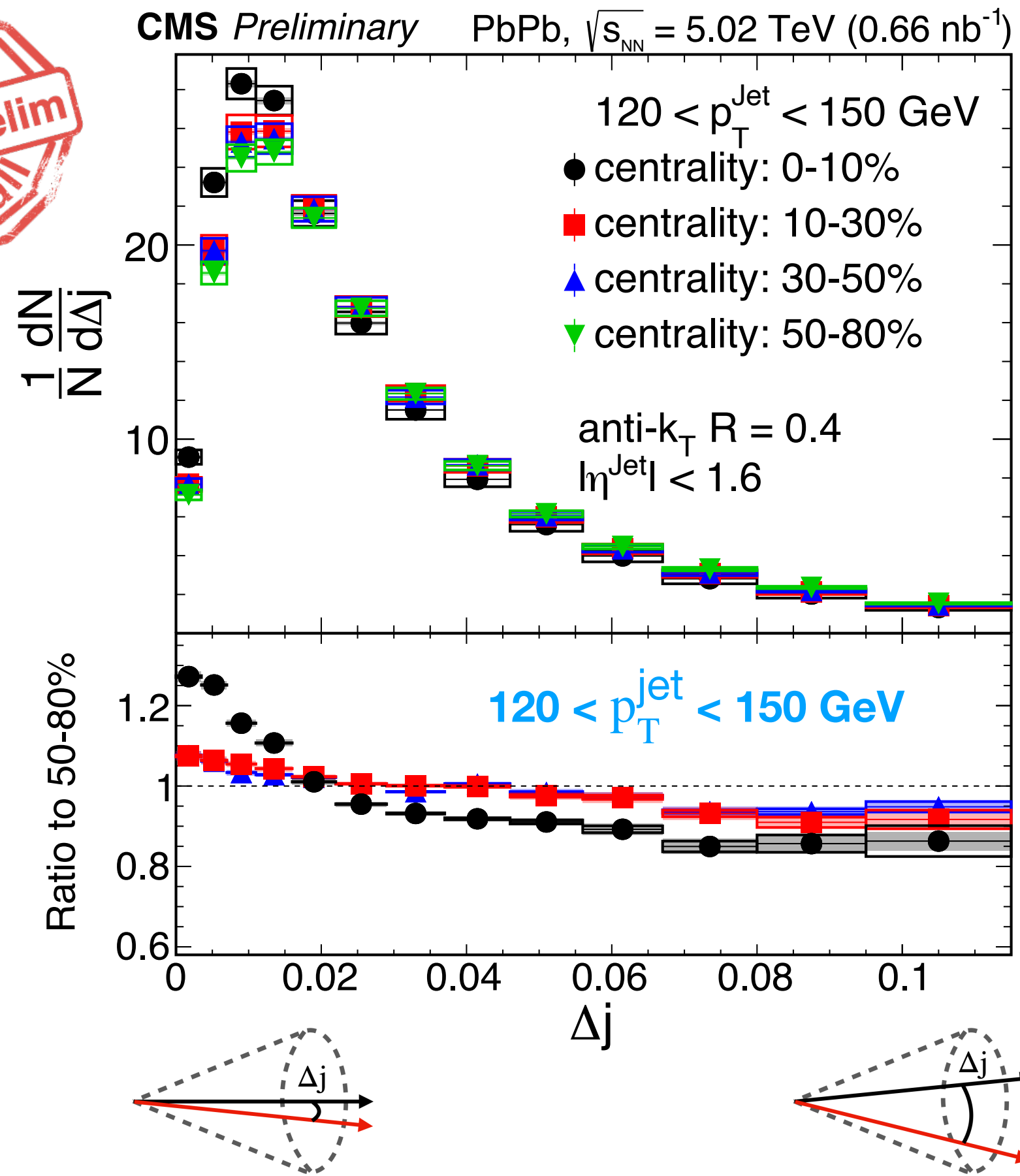


CMS PAS-HIN-24-010

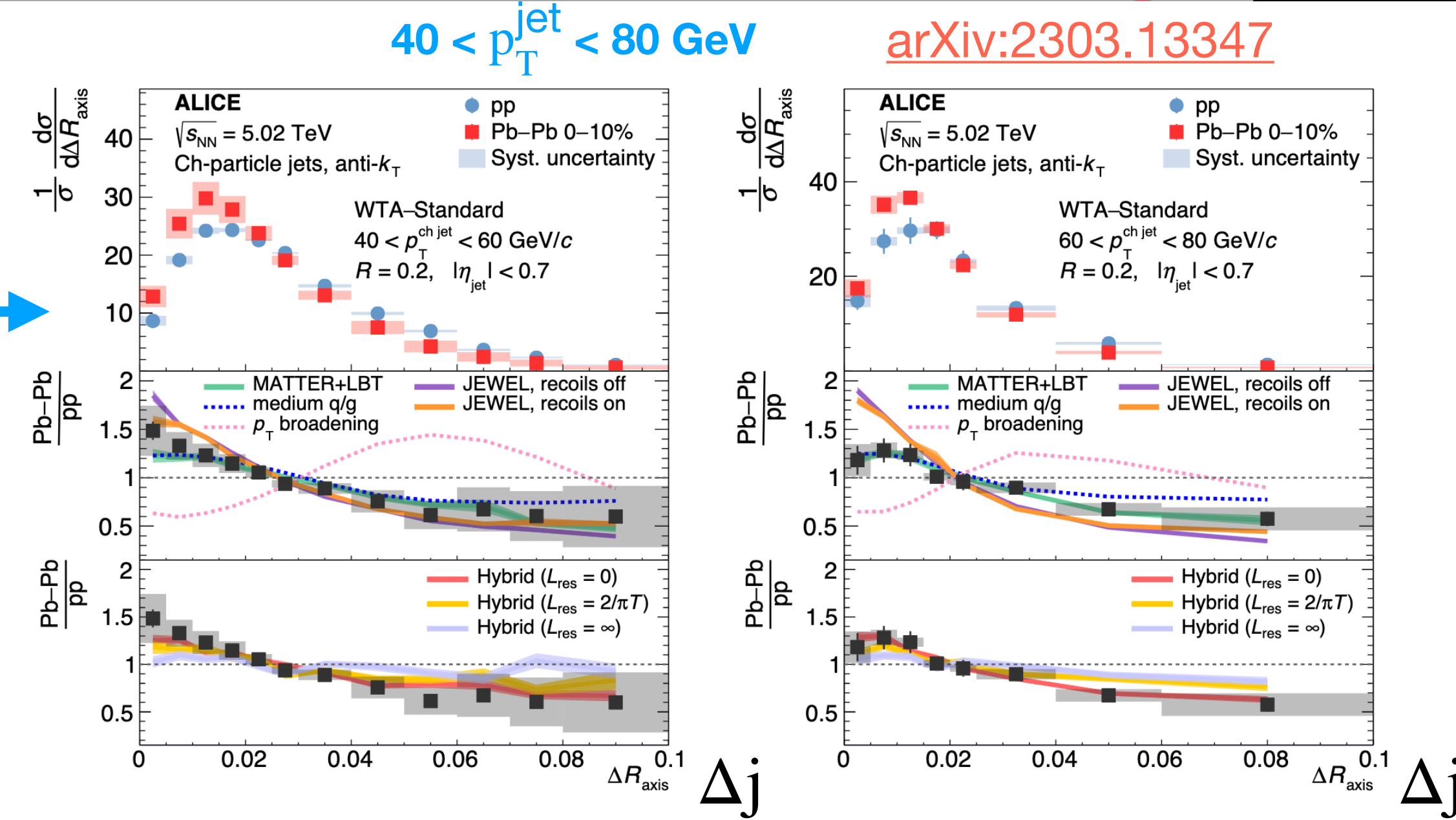
Comp. with previous measurements



CMS PAS-HIN-24-010

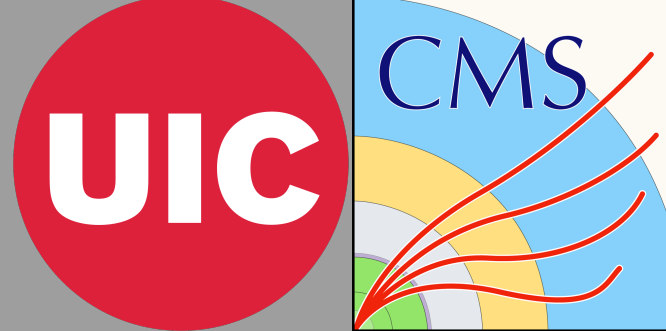


ALICE →

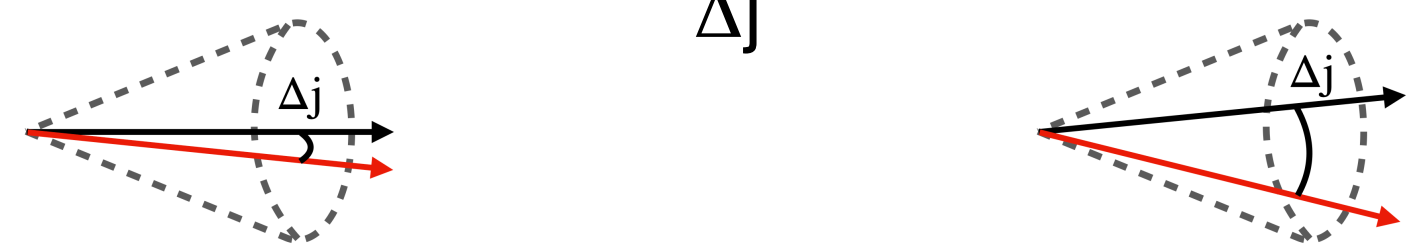
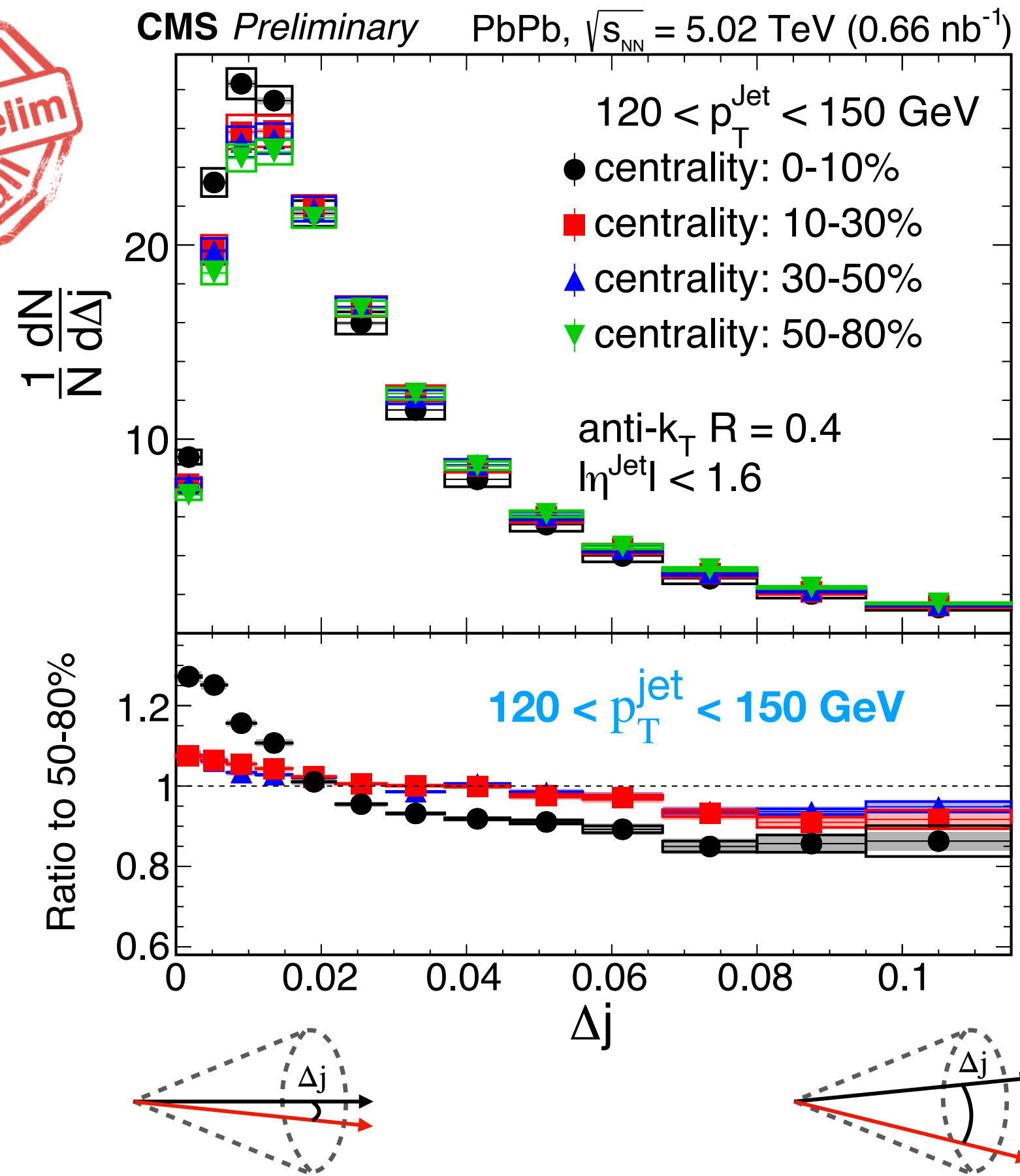


- Similar narrowing observed in ALICE inclusive measurement using charge jet

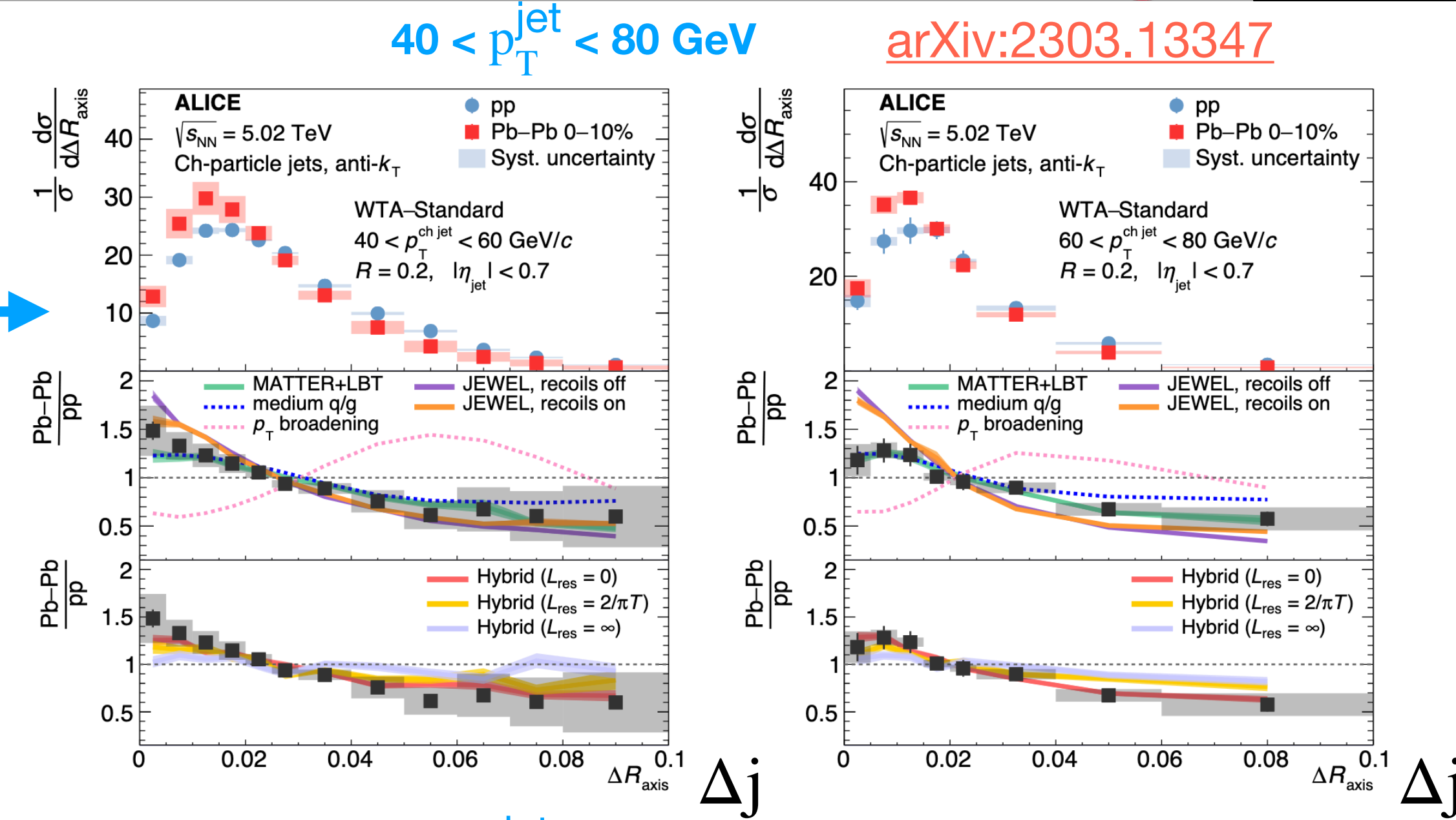
Comp. with previous measurements



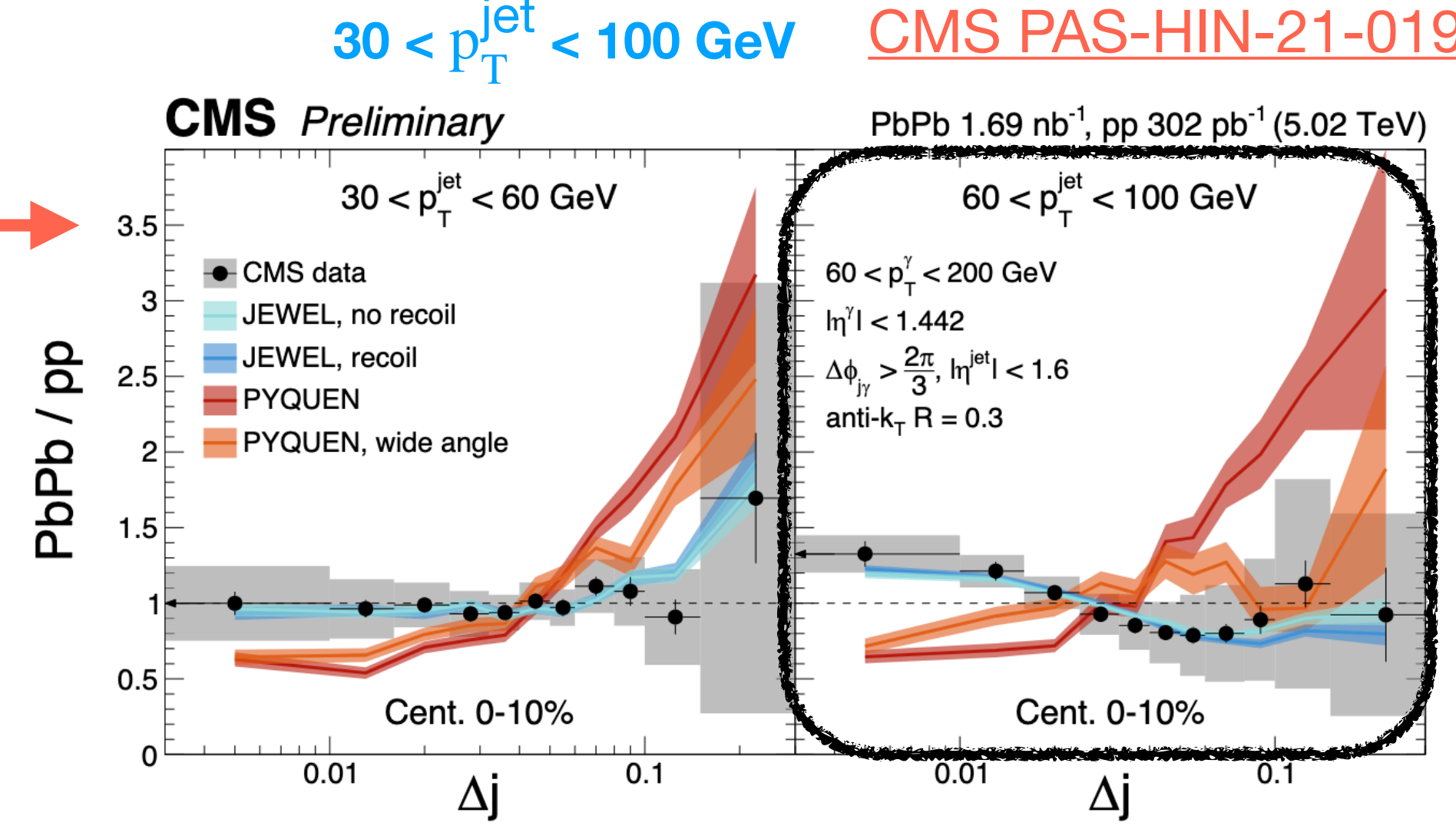
CMS PAS-HIN-24-010



ALICE →



CMS: See Molly Park's talk →

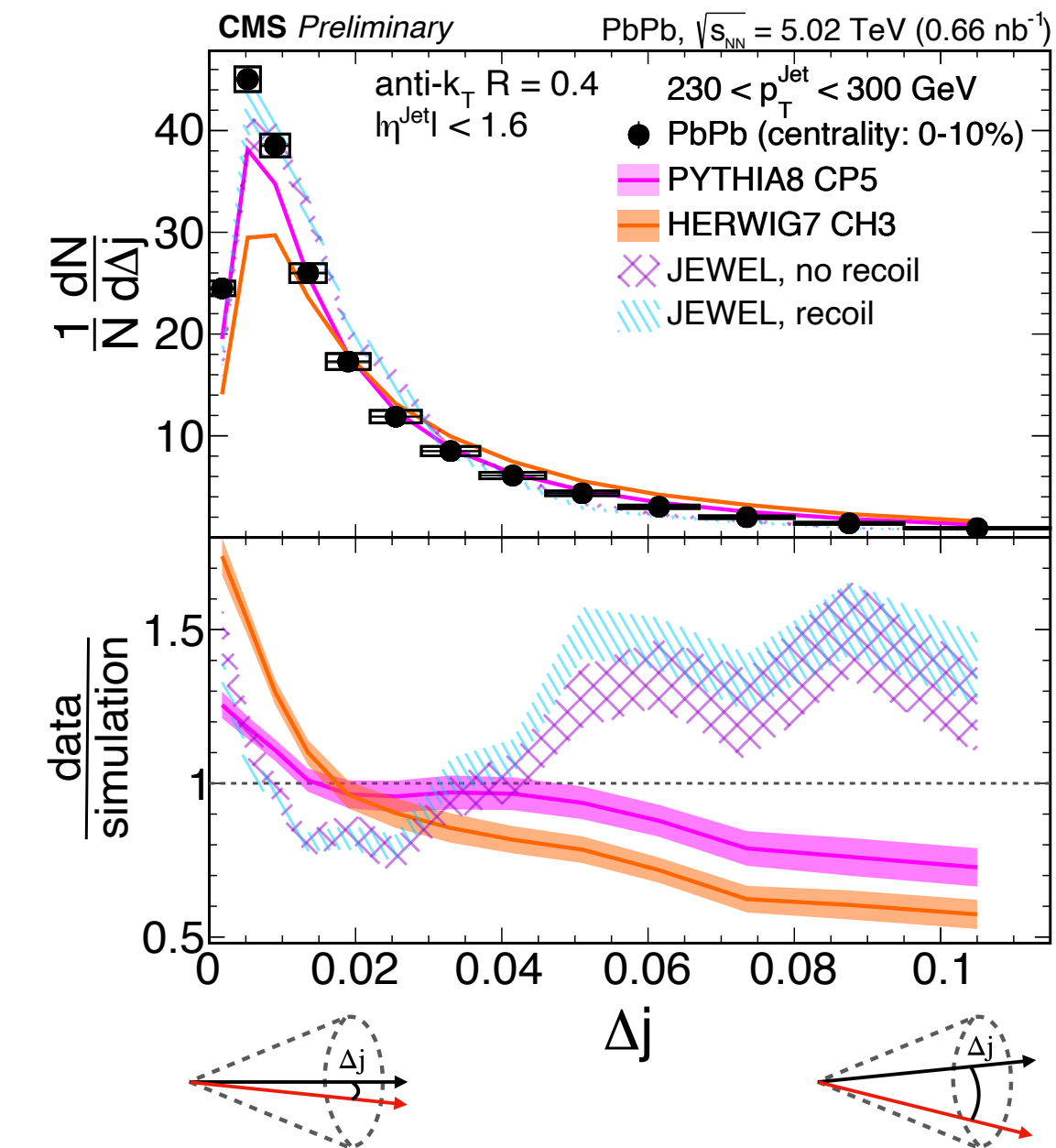
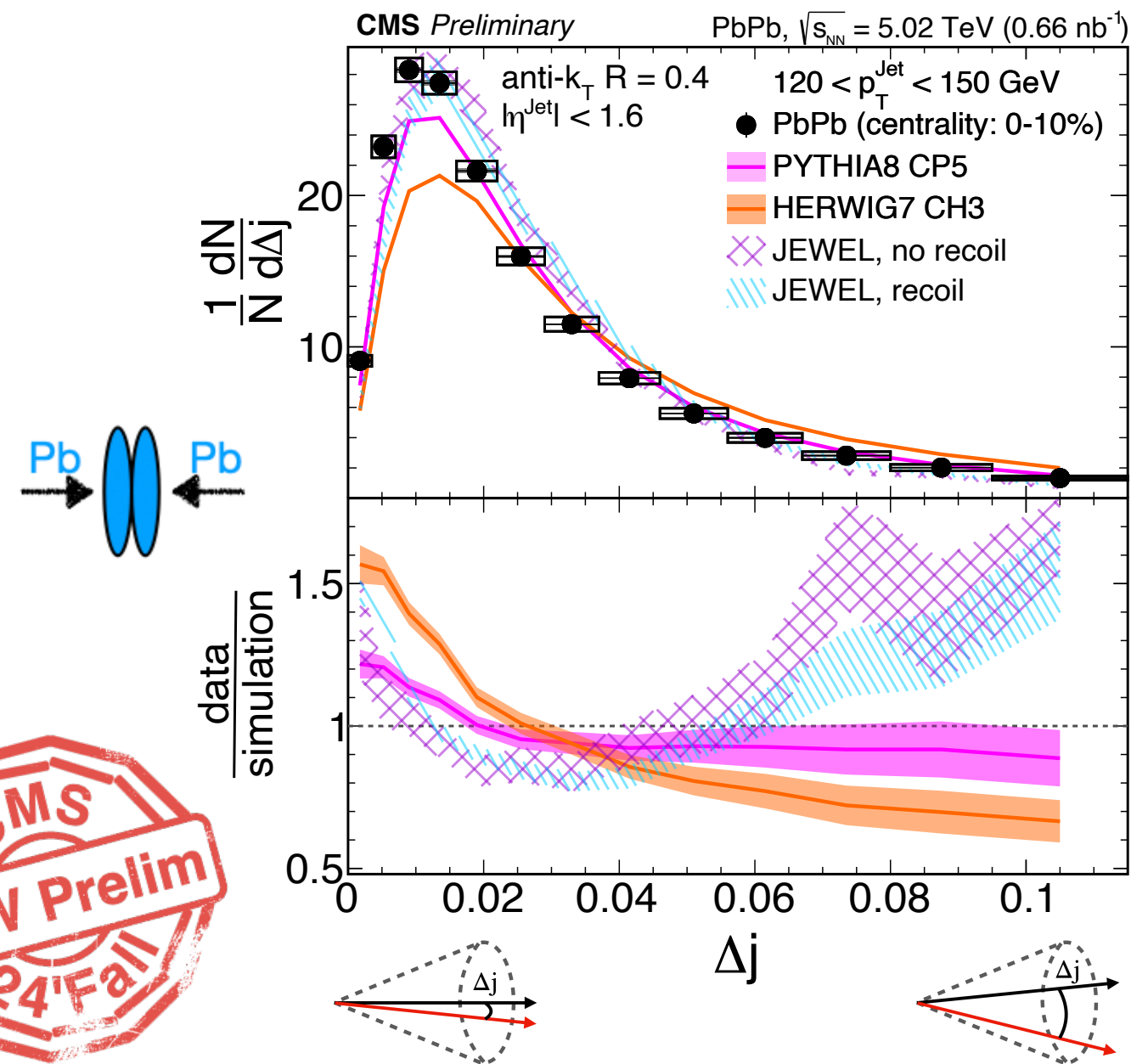
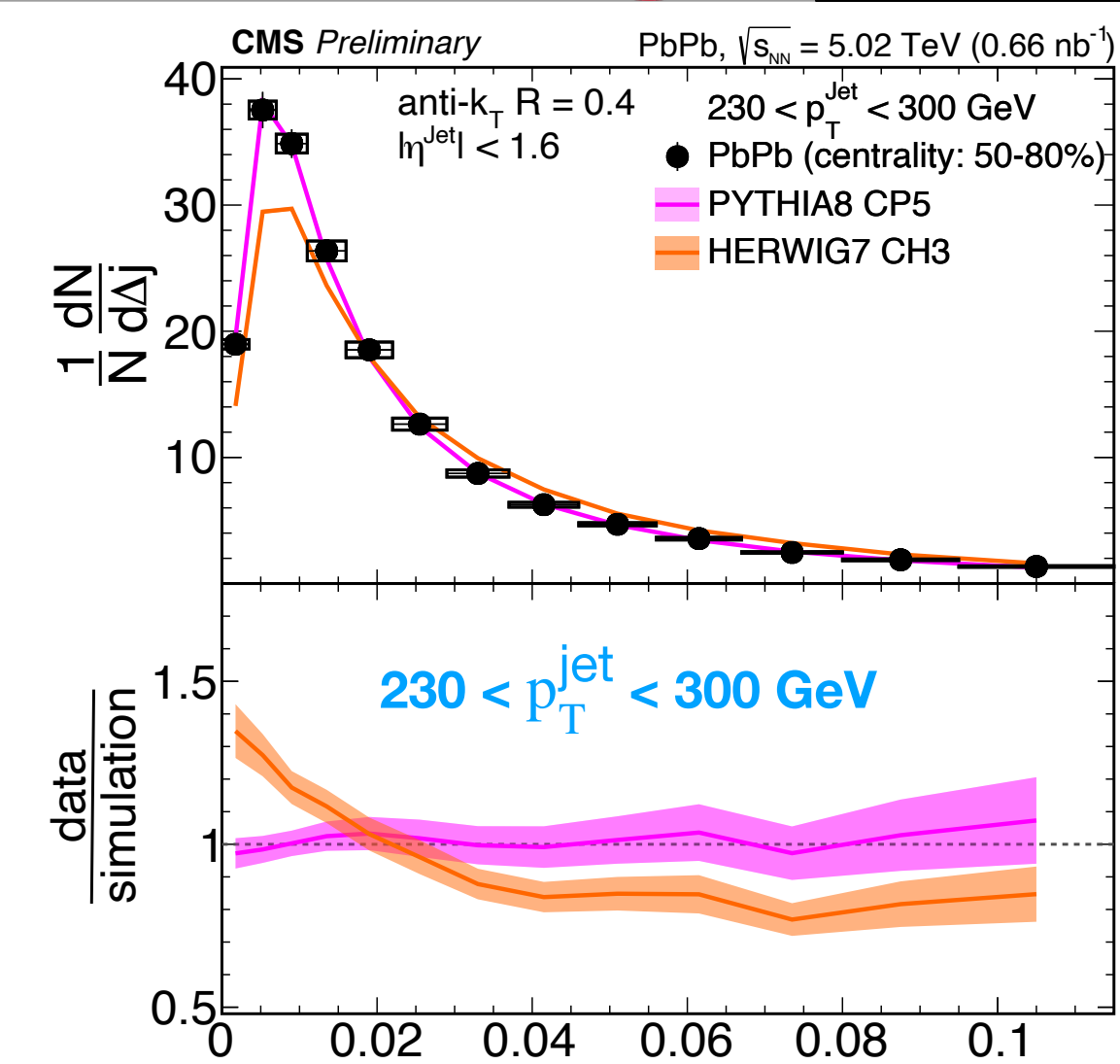
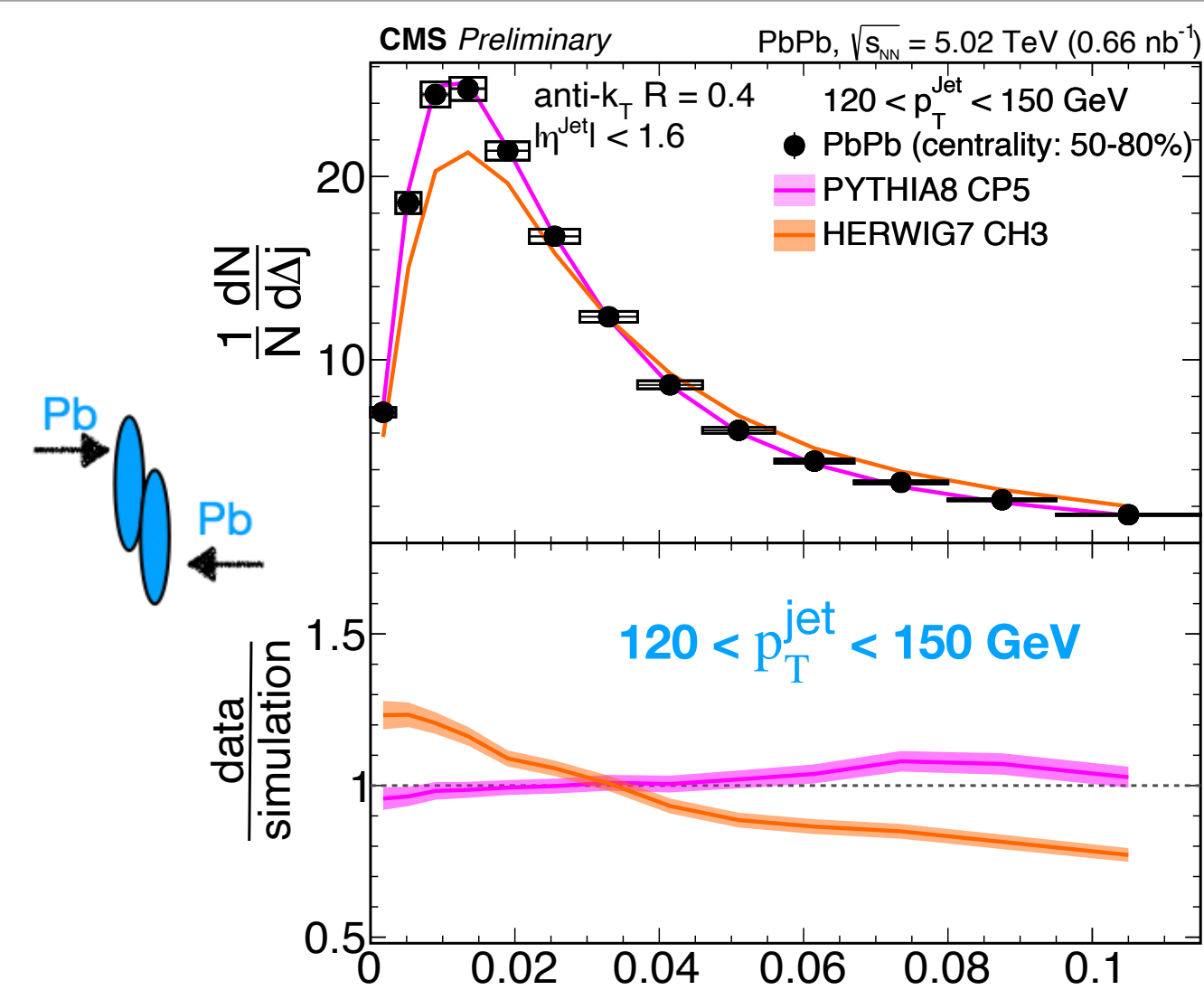


- Similar narrowing observed in ALICE inclusive measurement using charge jet
- Using γ +jet, CMS also observed narrowing in $60 < p_T^{\text{jet}} < 100$ GeV
- Not a apple to apple comparison, but physics observation is same

Models comparison



- Comparison with unquenched **PYTHIA** and **HERWIG**, and **JEWEL**
- **PYTHIA** describe well for peripheral 50-80% data, but fails to explain central 0-10% data as expected
- **HERWIG** has broader distribution compared to data
- **JEWEL** also fails to explain the central 0-10% data
- However, good to check the ratio between 0-10% and 50-80% in **JEWEL** (when it will be available) and then compare the same in data



CMS PAS-HIN-24-010



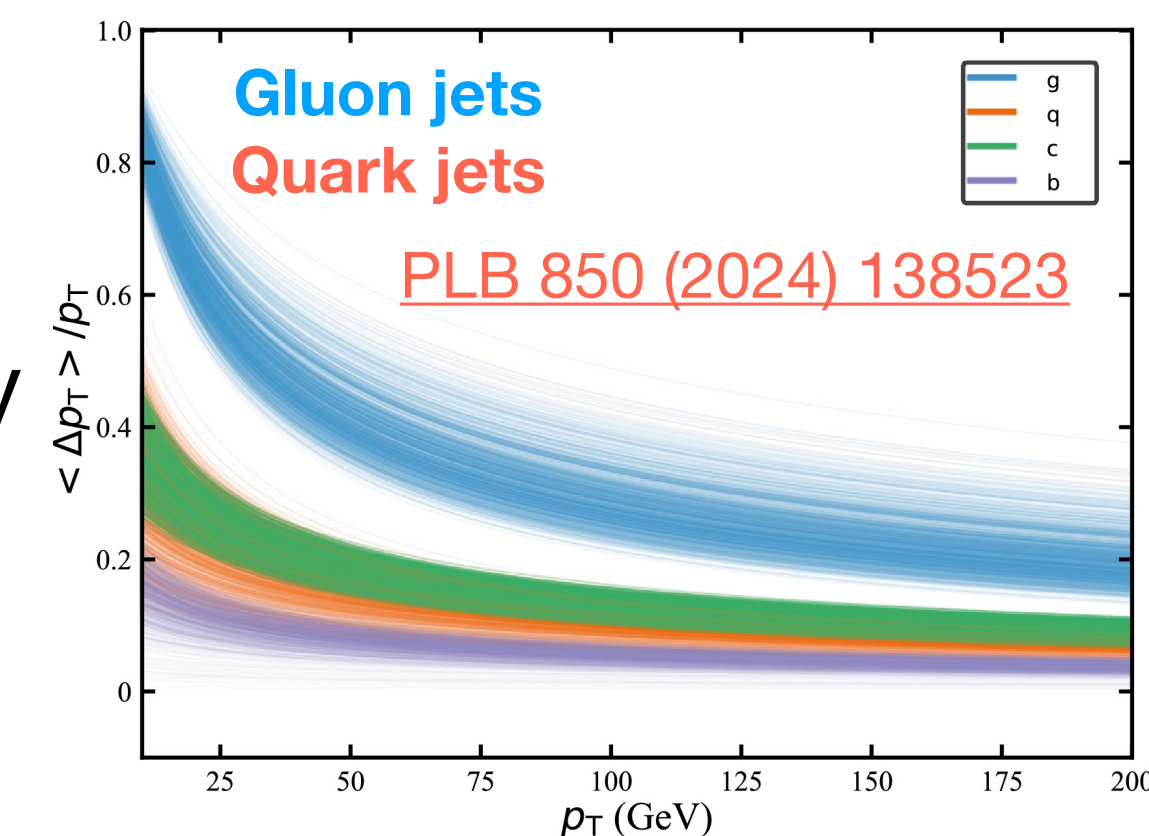
Models comparison continue..

Modified quark/gluon fractions in presence of medium using modified jet function:

[PRL 122 \(2019\) 252301](#)

Medium q/g: Reweight the vacuum PYTHIA based on modified quark/gluon fractions

- Color charge dependent energy loss
 - ▶ gluon jet lose more energy than quark jet



Models comparison continue..



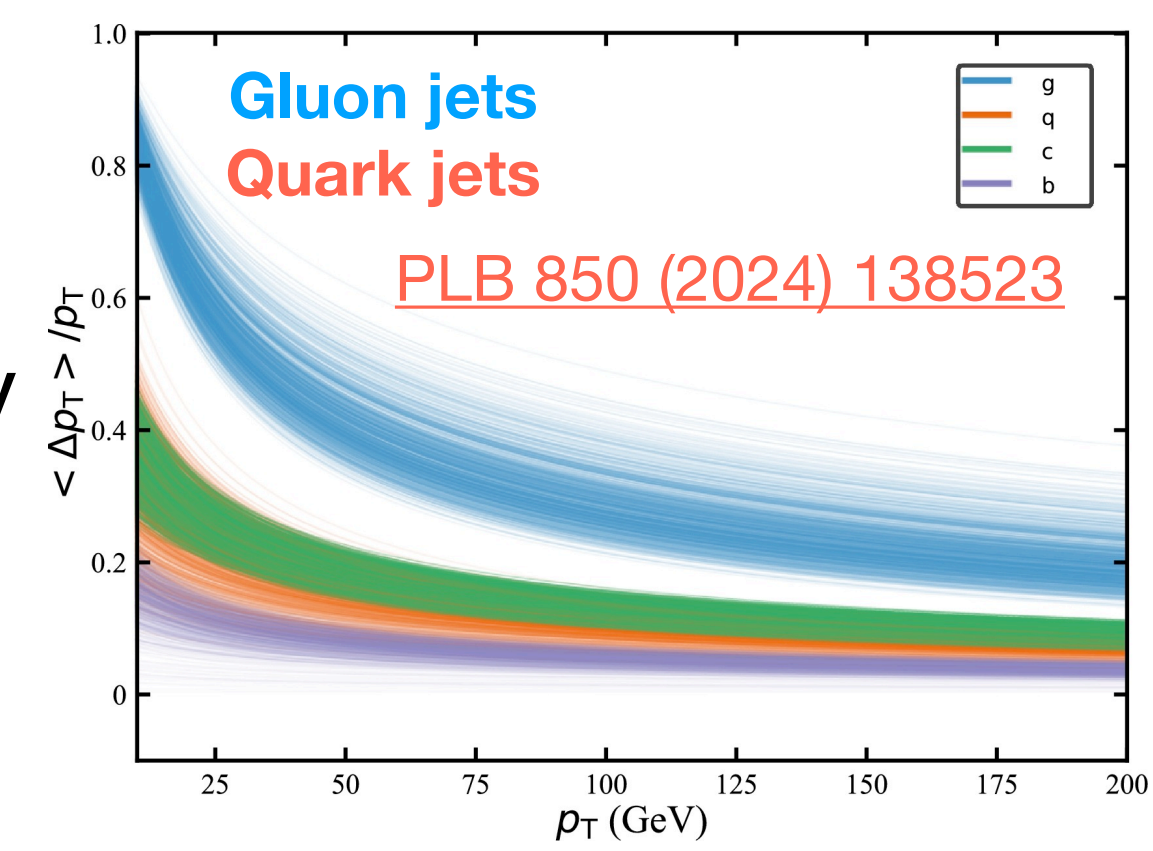
Modified quark/gluon fractions in presence of medium using modified jet function:

[PRL 122 \(2019\) 252301](#)

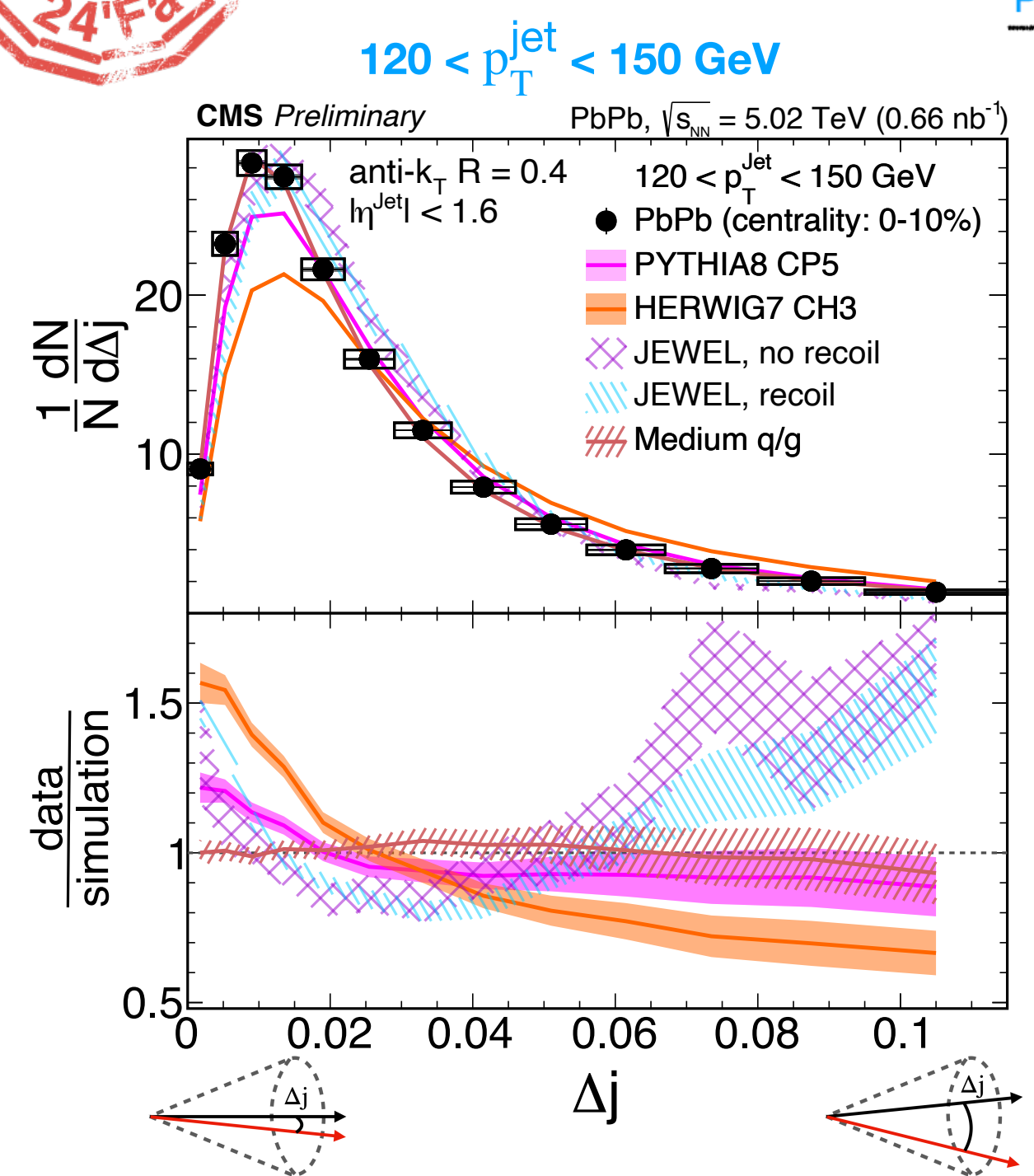
Medium q/g: Reweight the vacuum PYTHIA based on modified quark/gluon fractions

• **Medium q/g** describe well the low p_T central 0-10% data

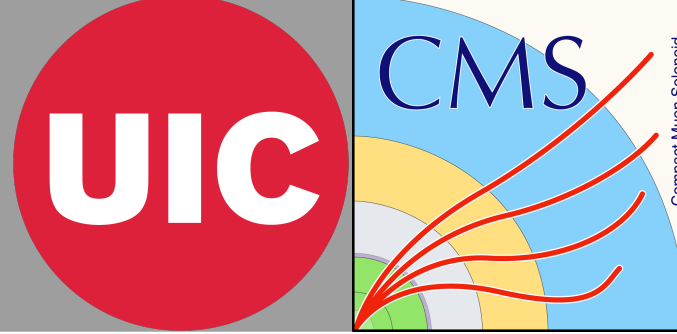
- Color charge dependent energy loss
 - ▶ gluon jet lose more energy than quark jet



CMS PAS-HIN-24-010



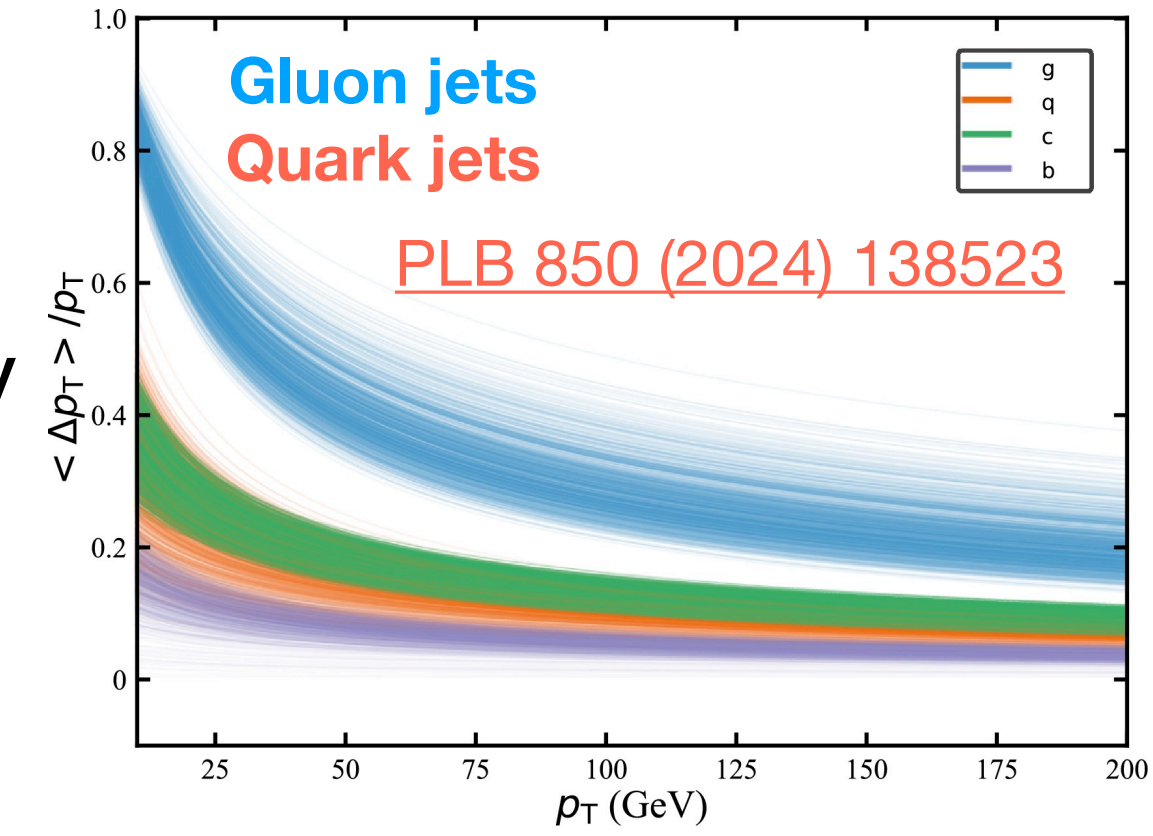
Models comparison continue..



Modified quark/gluon fractions in presence of medium using modified jet function:

[PRL 122 \(2019\) 252301](#)

- Color charge dependent energy loss
 - ▶ gluon jet lose more energy than quark jet

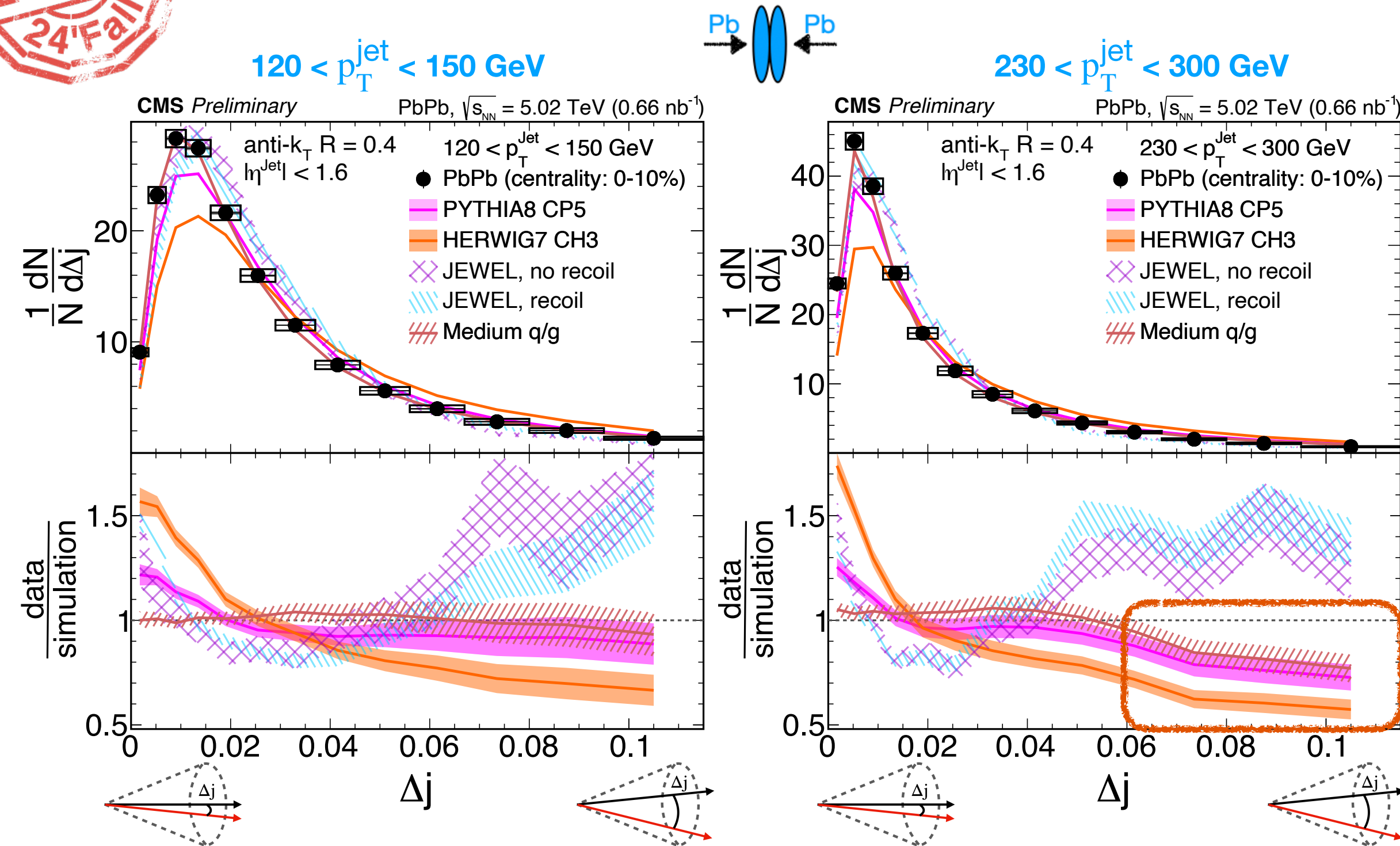


Medium q/g: Reweight the vacuum PYTHIA based on modified quark/gluon fractions



CMS PAS-HIN-24-010

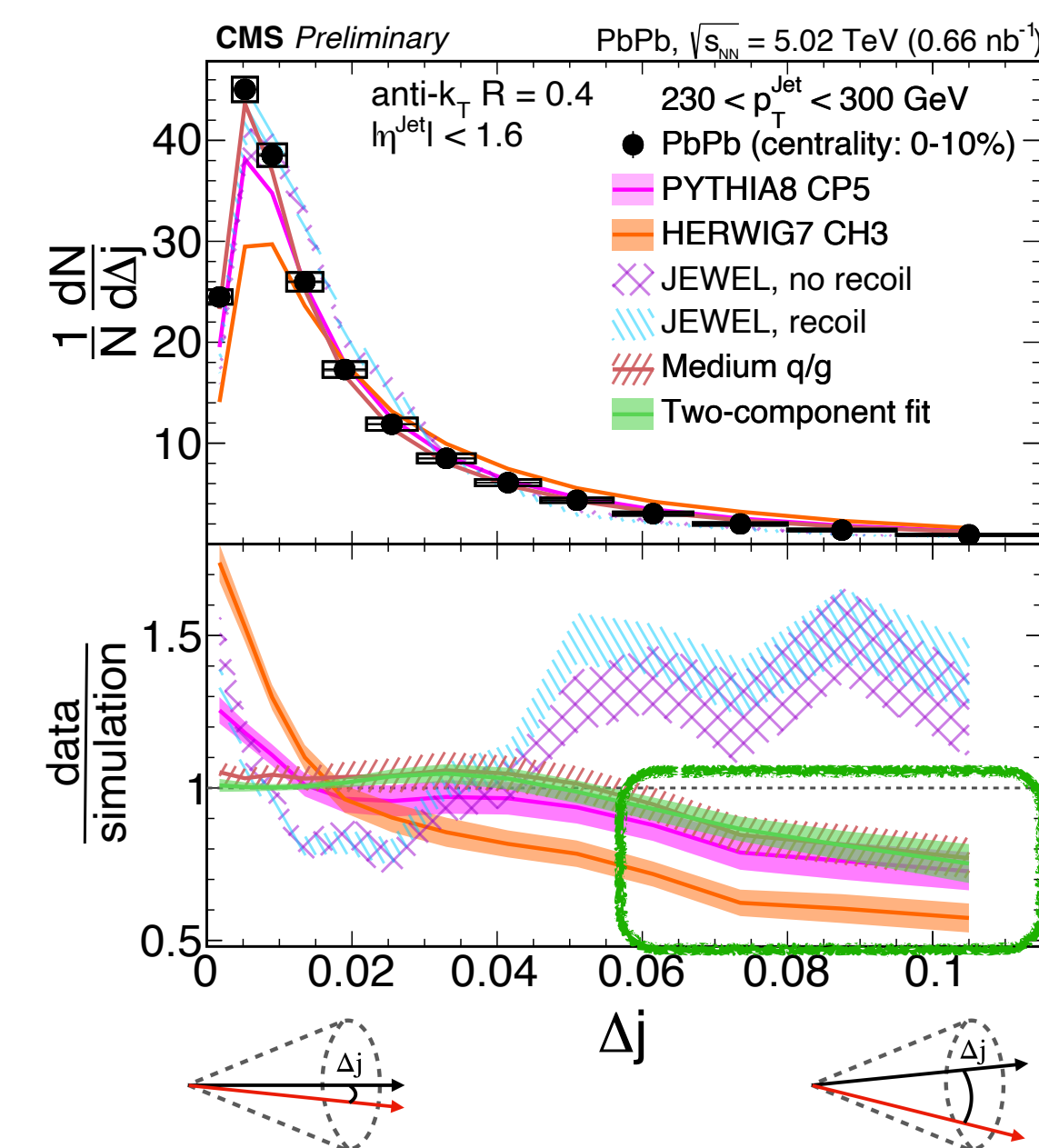
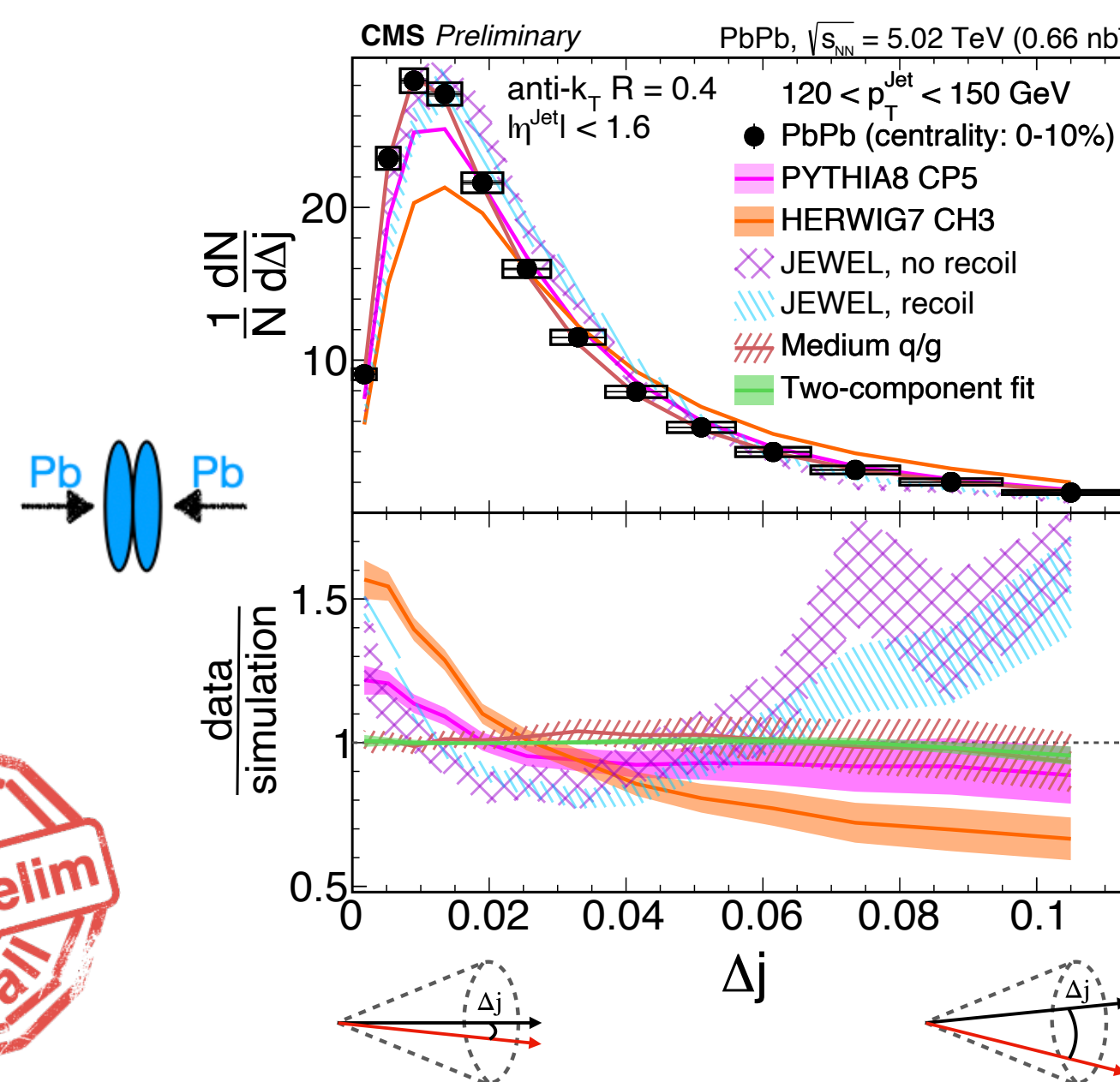
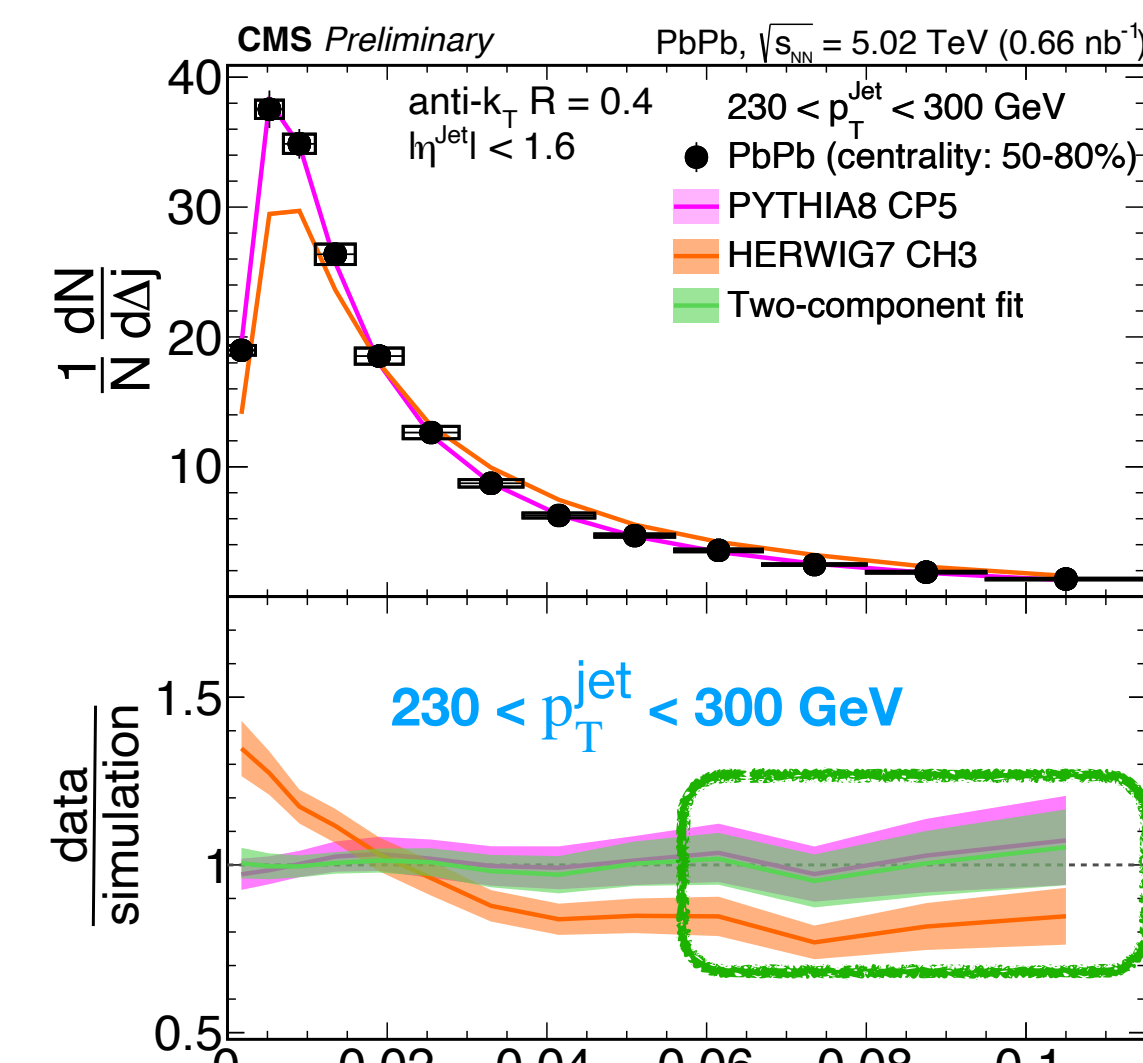
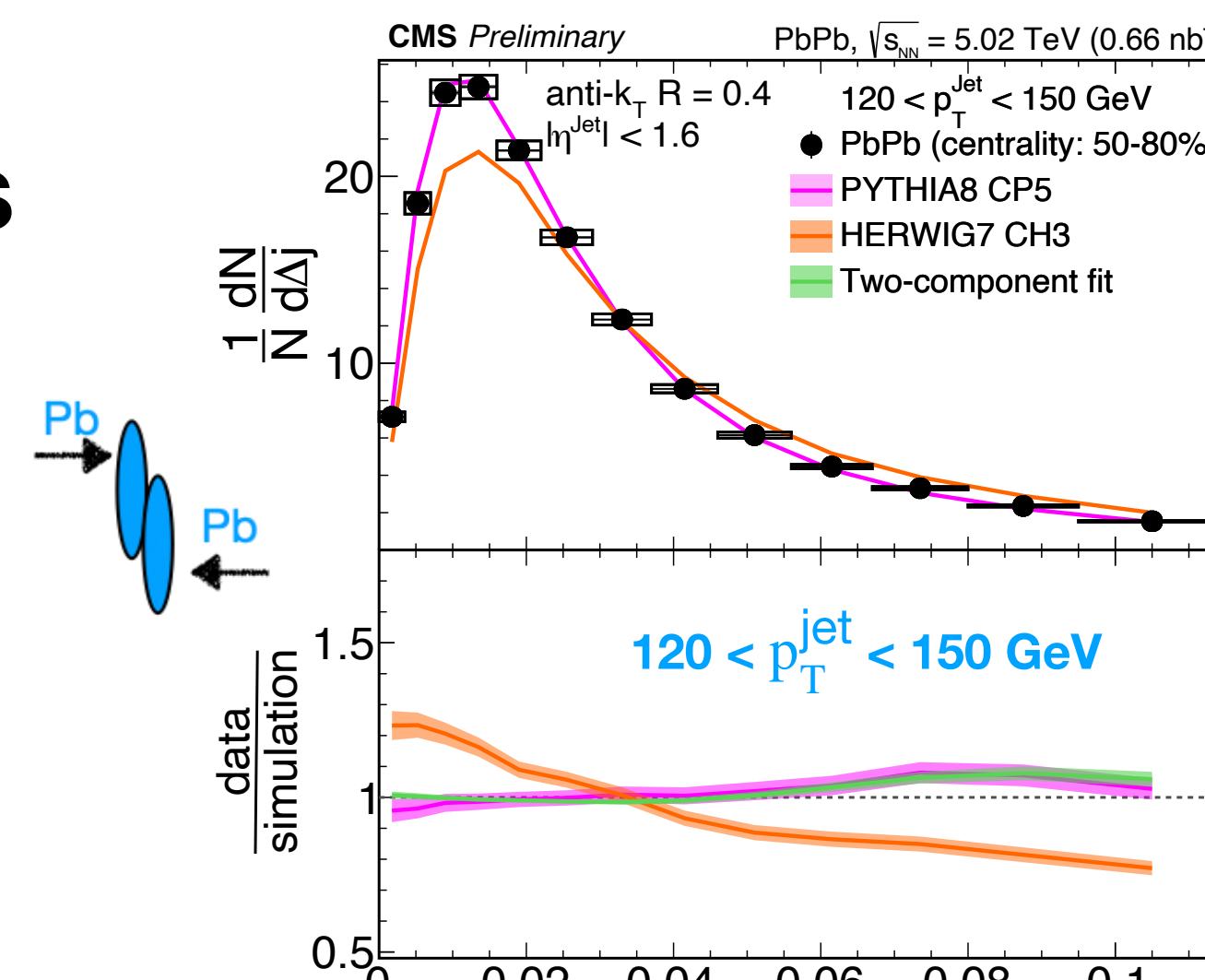
- **Medium q/g** describe well the low p_T central 0-10% data
- It fails to explain the high p_T central data, particularly towards high Δ_j
- I.e., only quark/gluon fractions change cannot explain this narrowing behaviour
 - ▶ Indicating the need to account for medium-induced substructure



Models comparison continue..

Further test on modified quark/gluon fractions

- **Two-component fit:** fit to unfolded data using vacuum PYTHIA quark and gluon templates
- The obtained gluon fractions in peripheral 50-80% aligns with PYTHIA expectations
- For central 0-10%, it is in excellent agreement with the prediction from **Medium q/g**
- Similar to **Medium q/g**, **Two-component fit** describe well the low p_T central 0-10% data, but fails to explain the high p_T central data, particularly towards high Δj



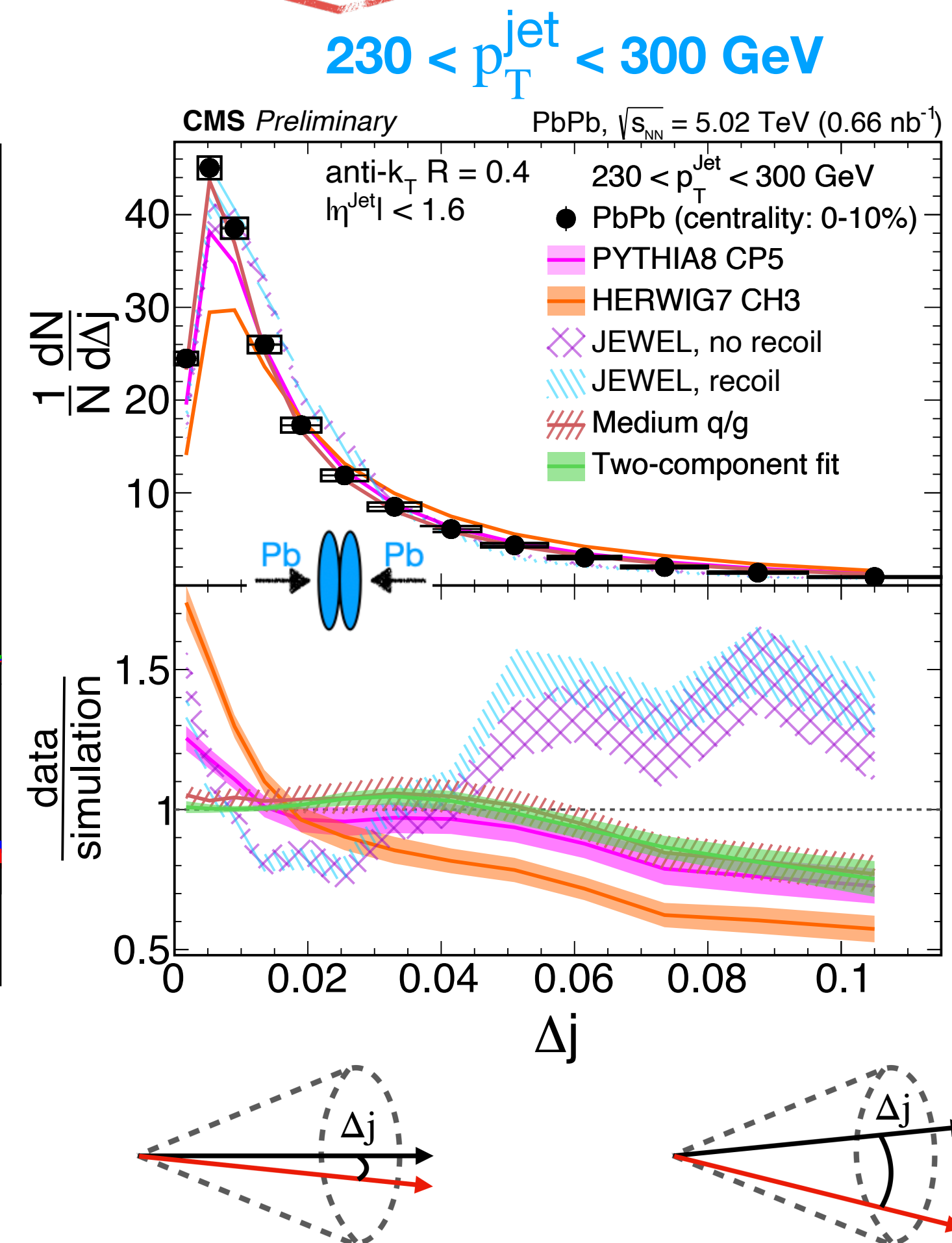
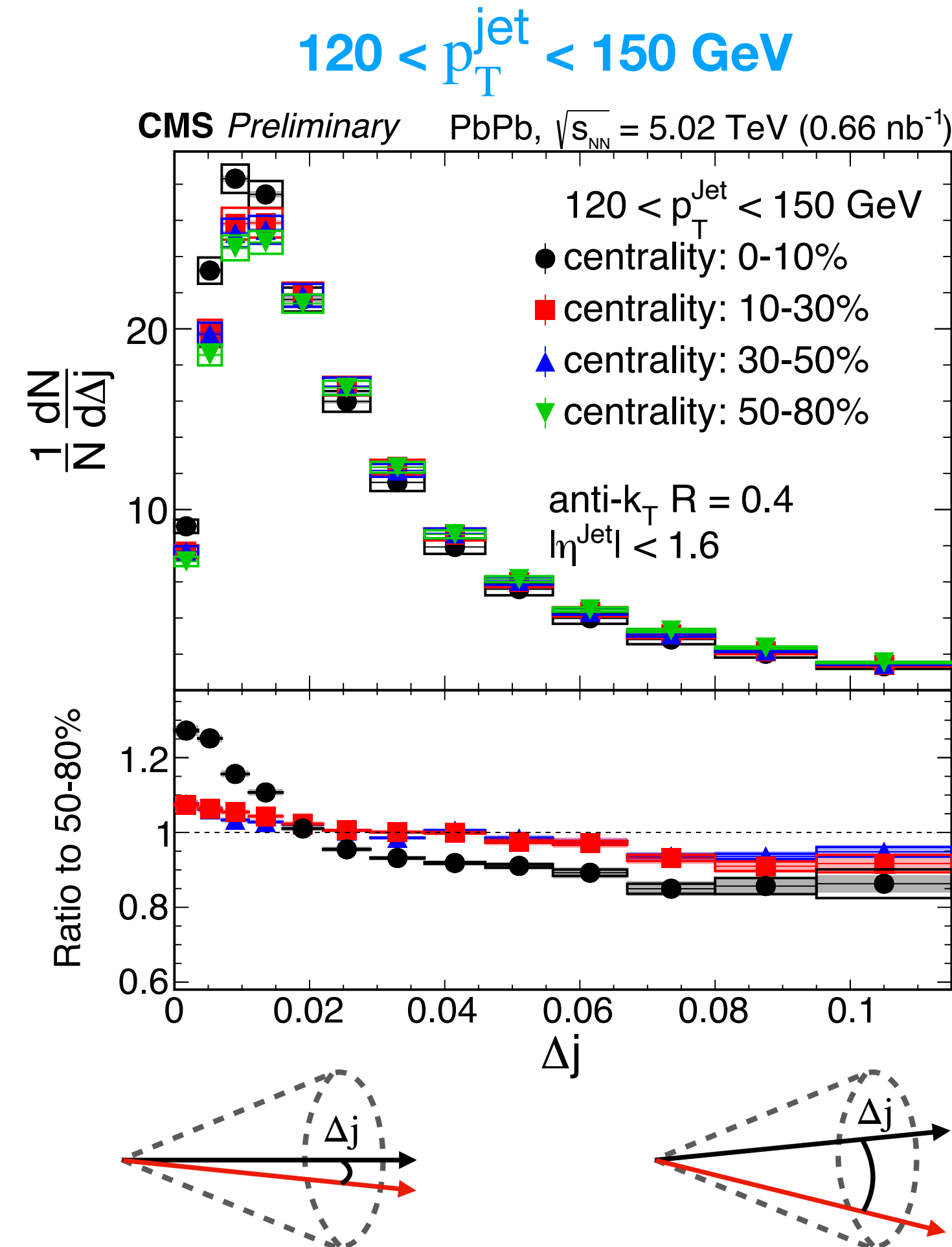
CMS PAS-HIN-24-010



CMS PAS-HIN-24-010



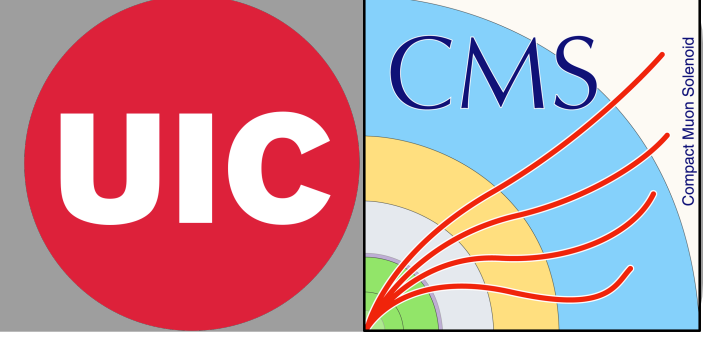
- The Δj distribution is narrower in central collisions than peripheral collisions in all the p_T^{jet} bins studied in this analysis
- Two energy loss models (**Medium q/g** and **Two-component fit**) fail to explain high Δj behaviour for high p_T^{jet} in the 0-10% central data
 - Indicates the need to account for medium-induced substructure modification



Thank you for your kind attention!



Backup



JES uncertainty : up and down [(anti)correlated with Δj]
JER uncertainty : centrality independent (JER up and down), centrality dependent [(anti)correlated with Δj]

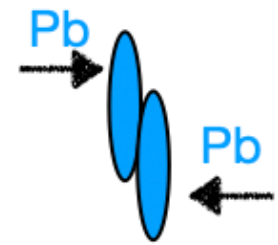
Background subtraction : akFlowPuCs4PF jets collection
Unfolding iteration : varied to 2 and 4
Response matrix statistics : using 50 toy response matrices
Modified template : reweight the response matrix and modify the quark gluon template based on the fraction extracted from raw data
Unfolding prior : generate new response matrix without pT reweight
Centrality variation : up and down

Correlated source

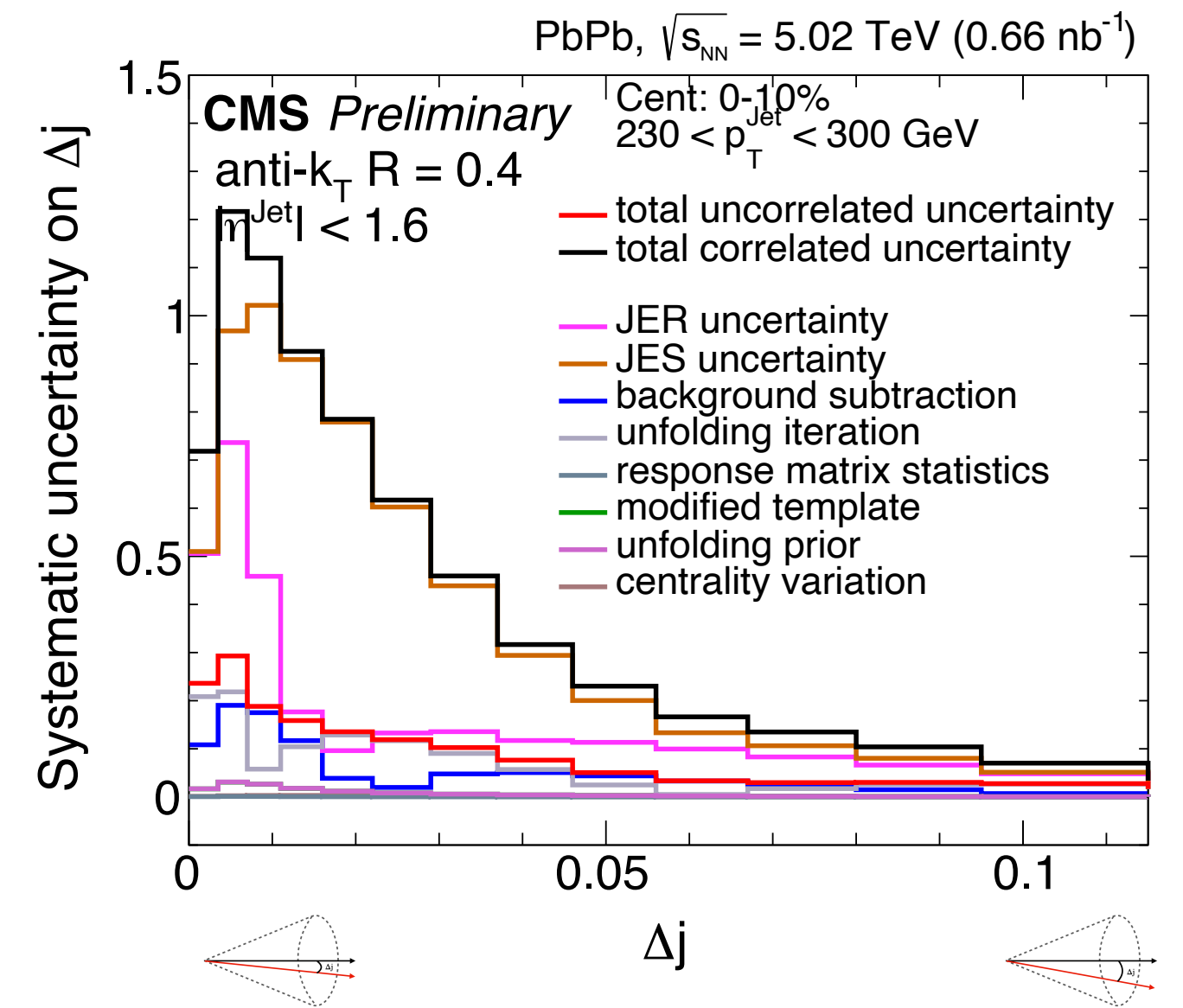
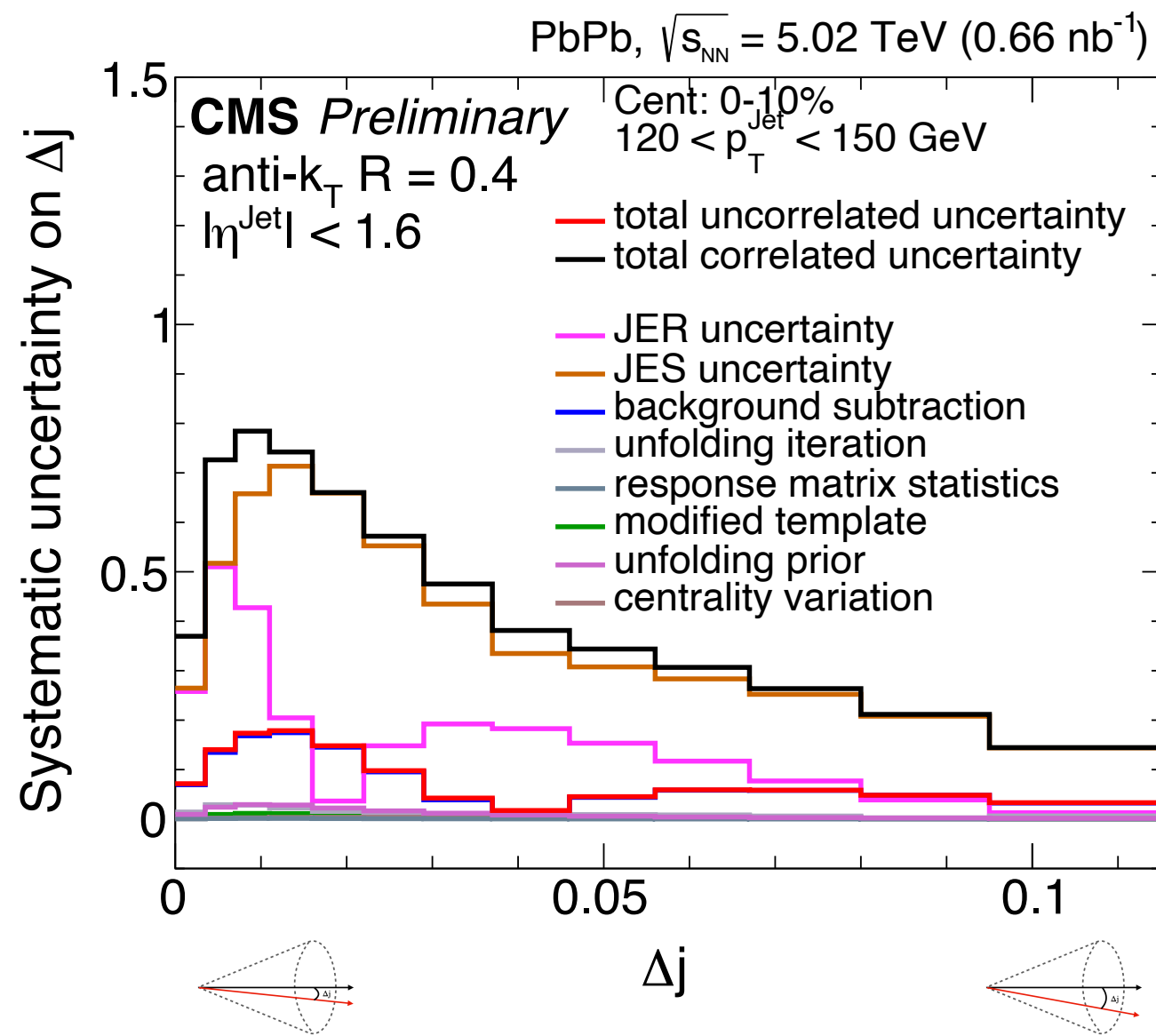
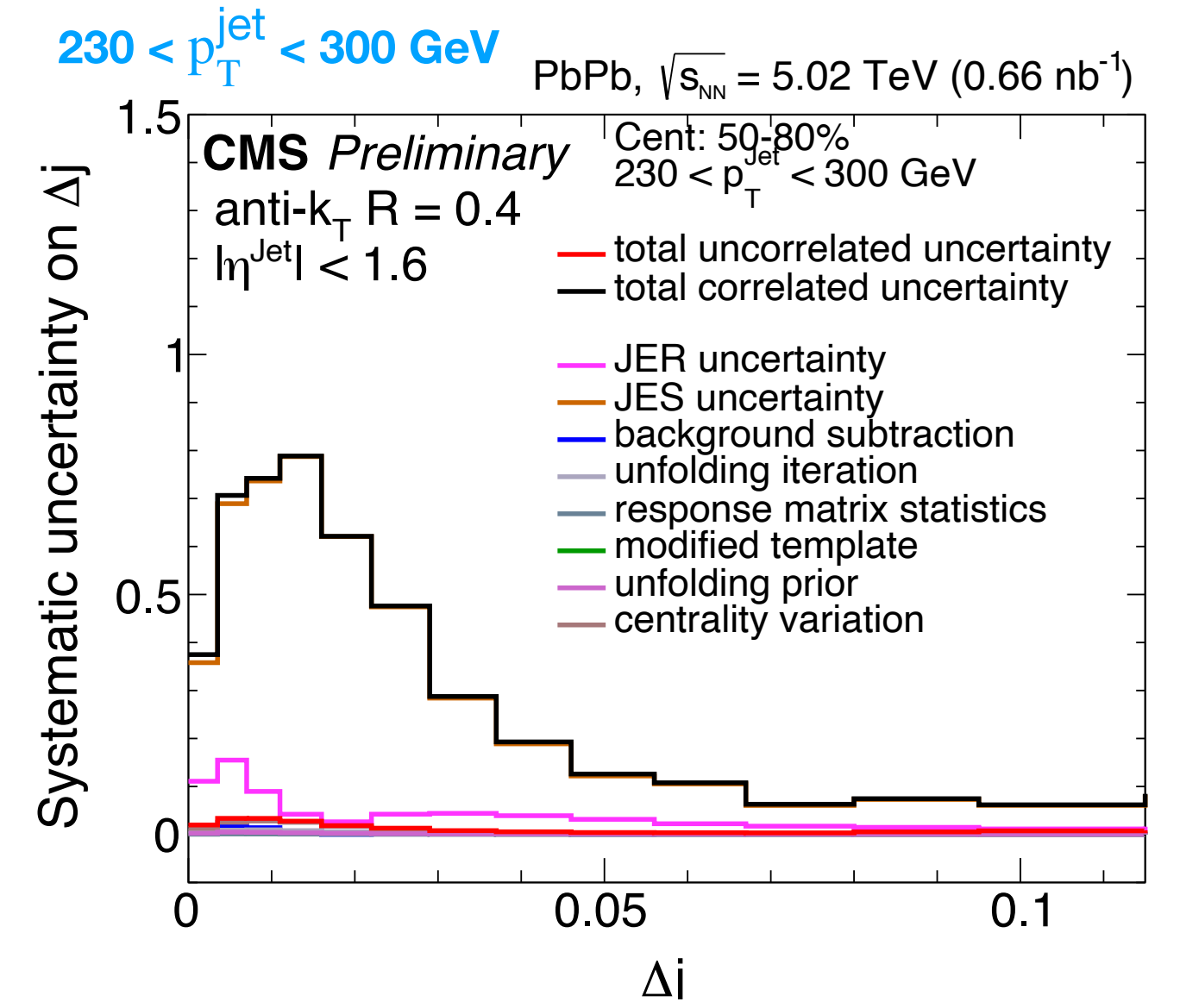
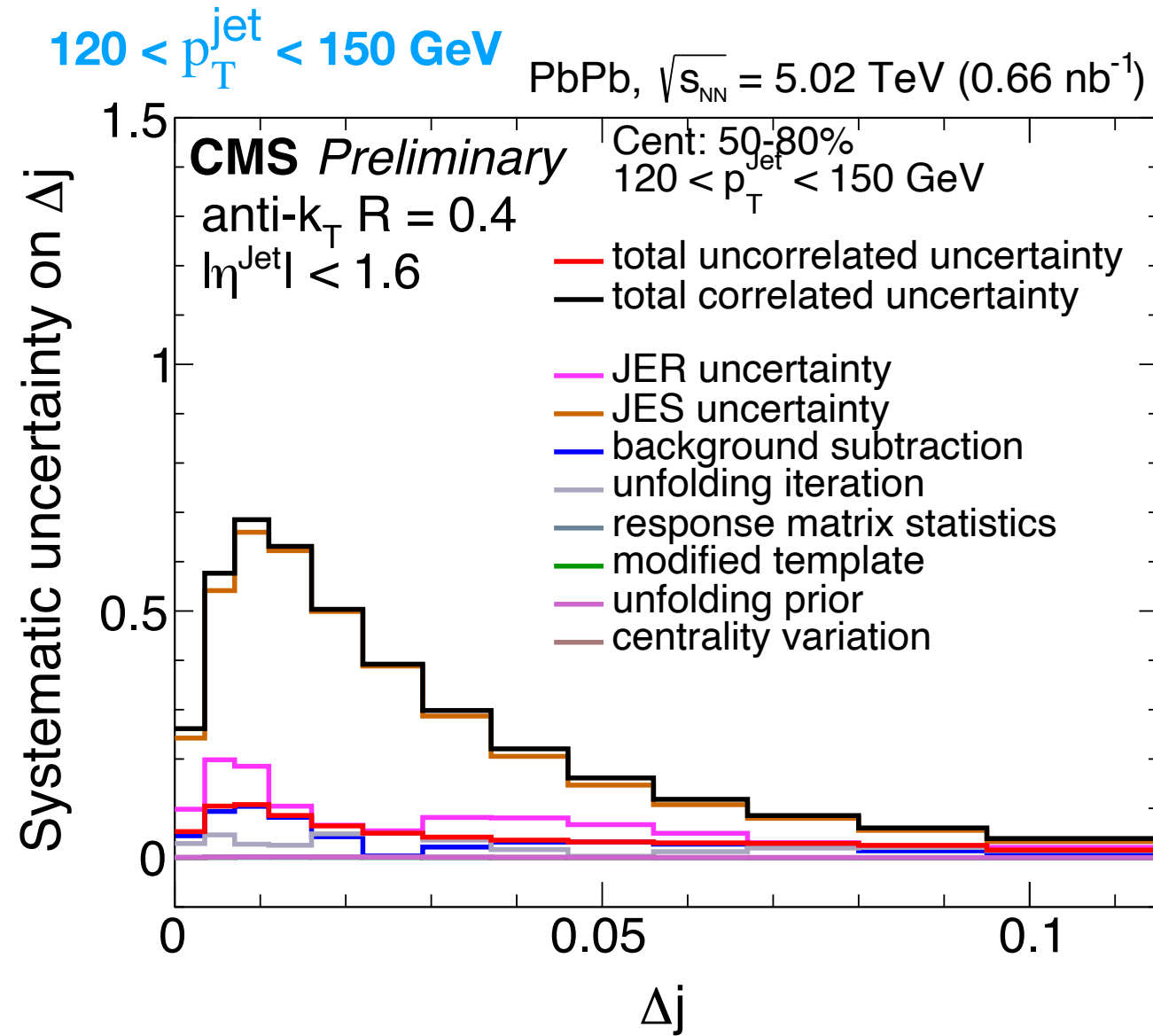
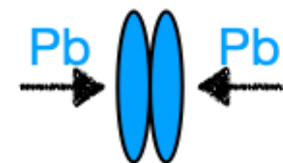
Uncorrelated source

Systematic uncertainty for Δj

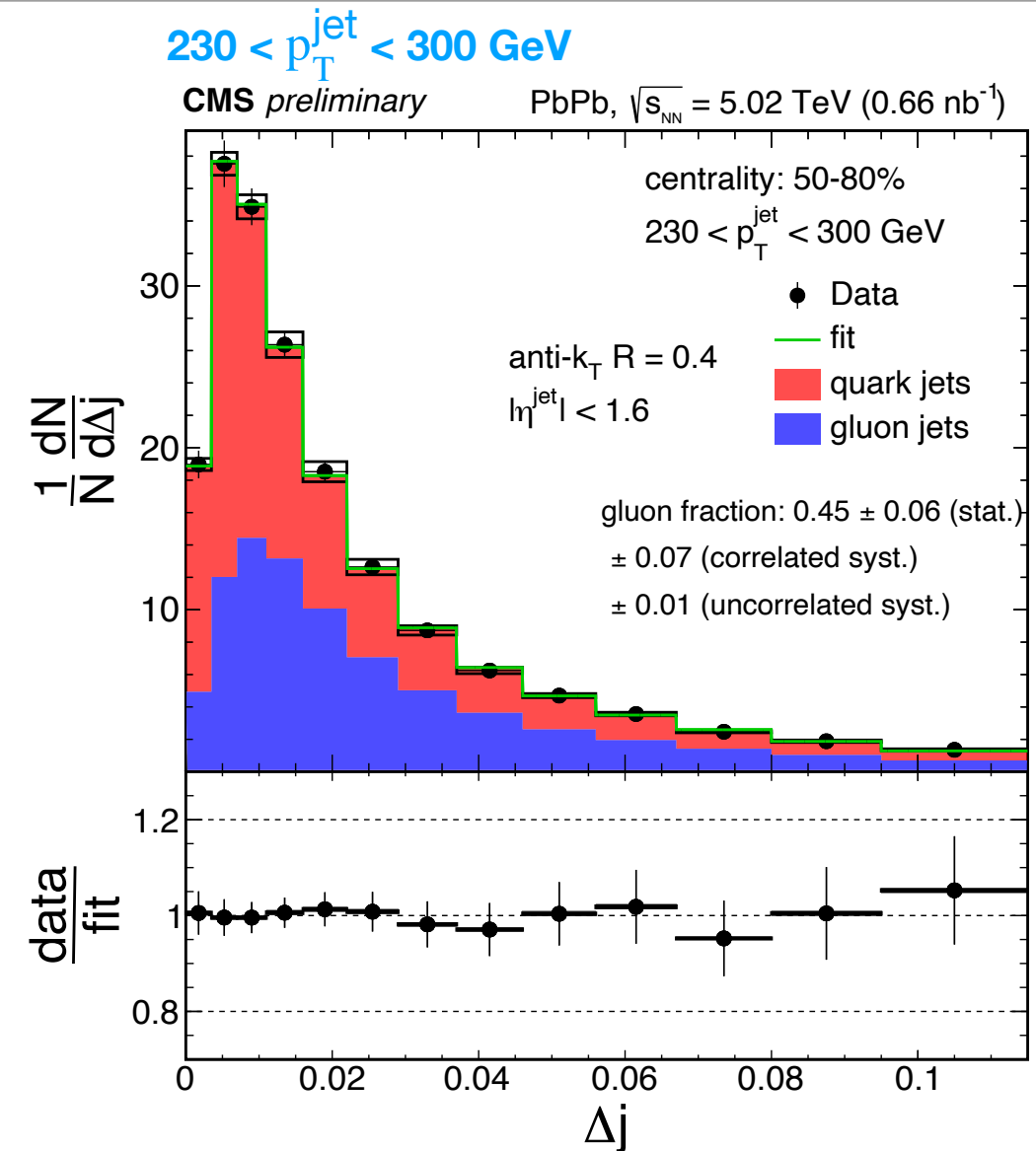
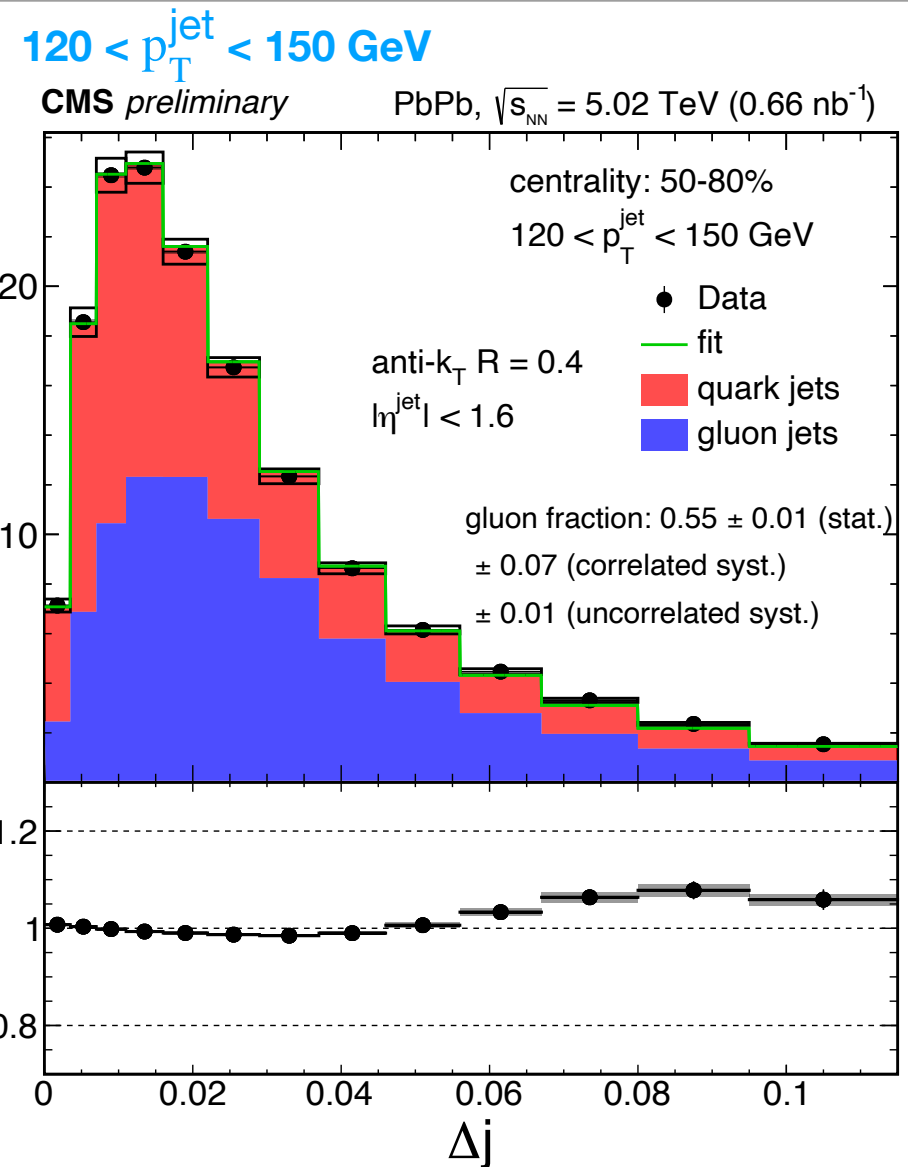
Absolute systematic uncertainty



- **JES** and **JER** are the dominant systematic for this analysis, which are also treated as correlated uncertainty
- Others are sub-dominant and treated as uncorrelated uncertainty



Template fit to data



Using vacuum PYTHIA

Δ_j is sensitive to parton flavour

